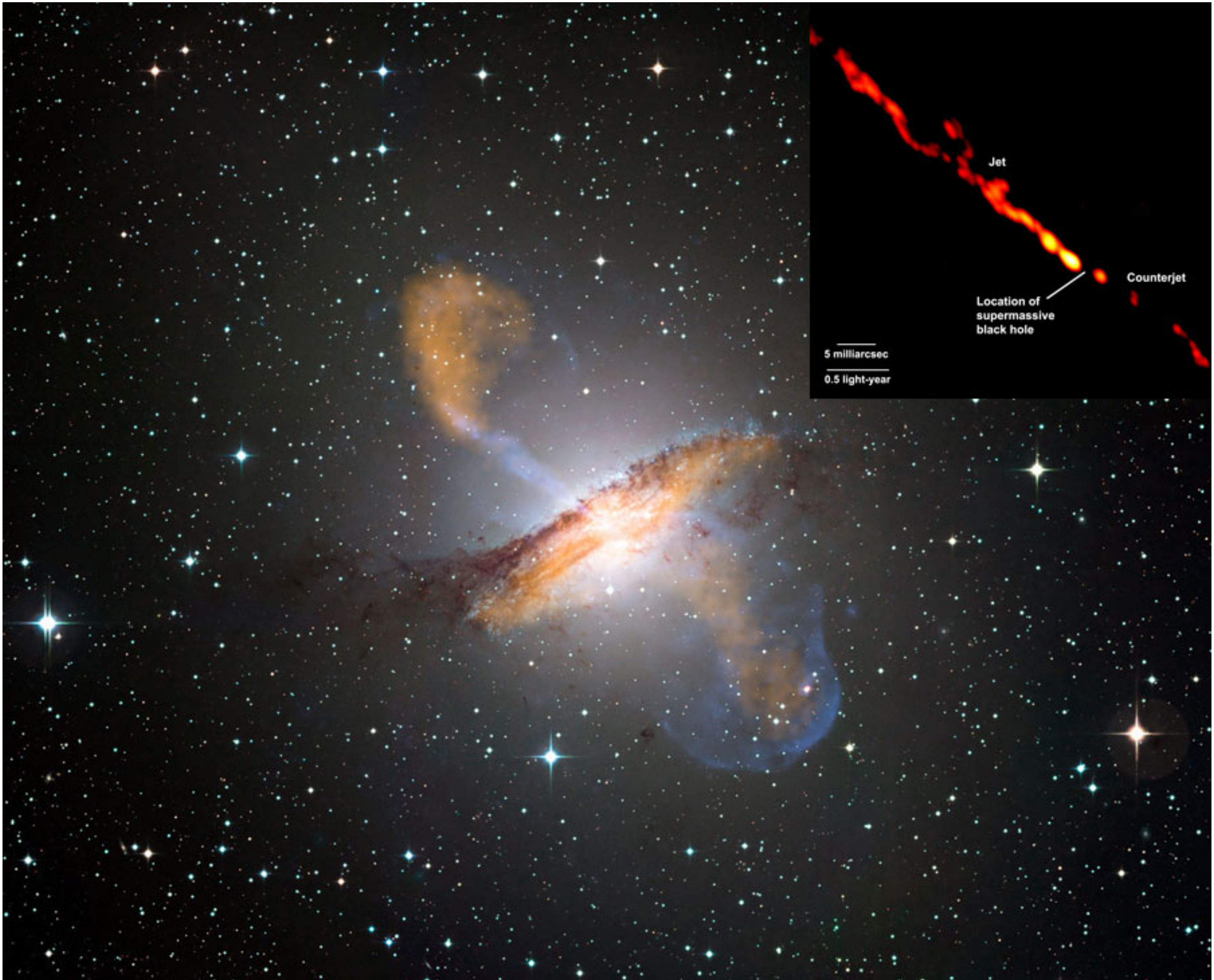

Jet
Counterjet
Location of supermassive black hole
5 milliarcsec
0.5 light-year

AGN physics in the age of Fermi

Fermi Summer School
Lewes, DE, 13-17 September, 2010

Chuck Dermer
United States Naval Research Laboratory
Washington, DC USA
charles.dermer@nrl.navy.mil

On behalf of the **Fermi Collaboration**

Outline

1. Radio Galaxies, Blazars, and Unification
2. Blazar Sequence
3. SED: Two Component Paradigm
4. Jet Physics: γγ opacity and synchrotron/SSC model
6. External Compton scattering processes
7. Variability

Blazar 3C 454.3's Record Flare

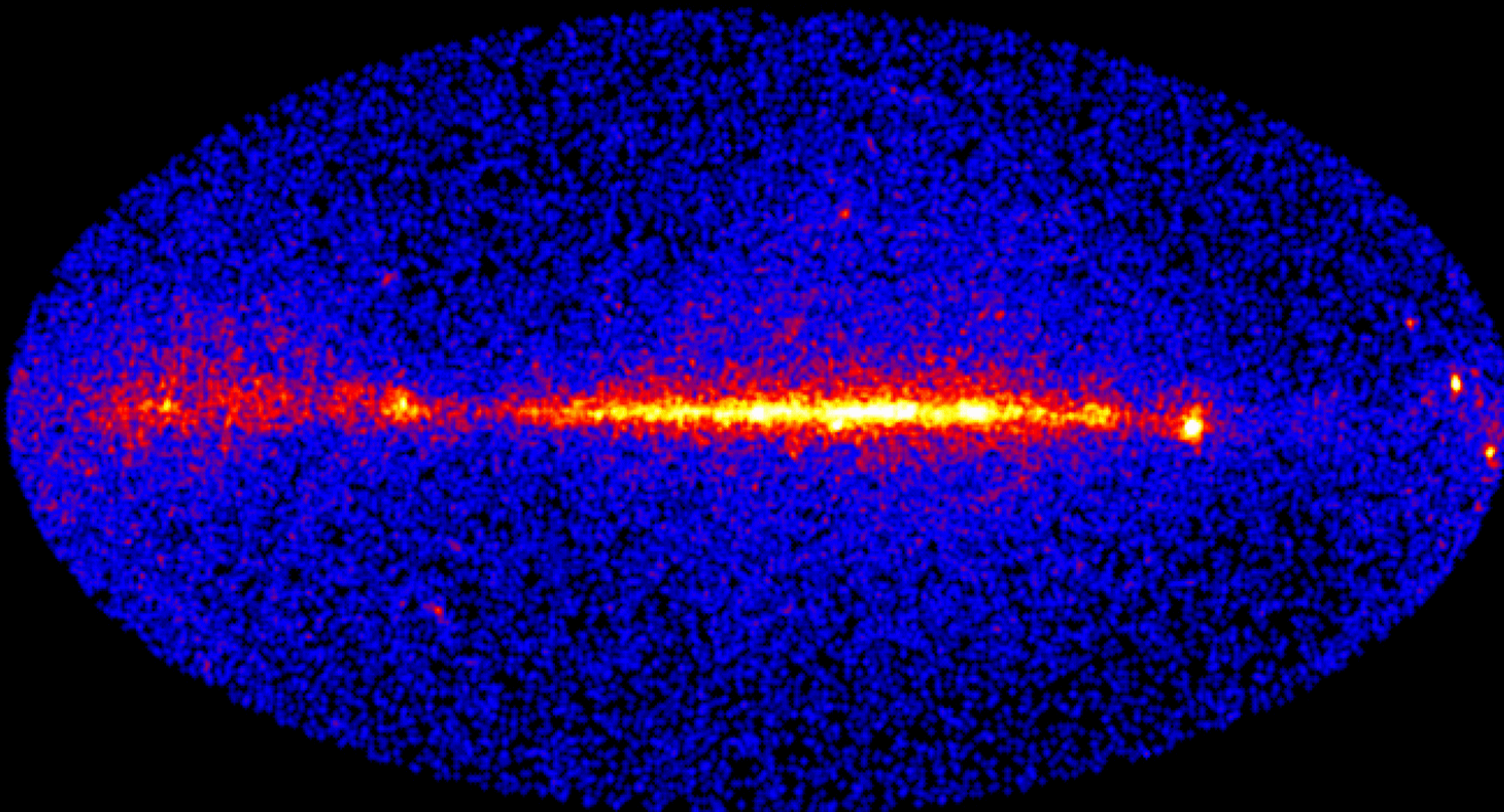

November 3, 2009

fermi
Gamma-ray
Space Telescope

Fermi AGNs

- LAT Bright AGN Sample (LBAS); First year LAT AGN Catalog (1LAC)

LBAS: 3 month source list: 2008 Aug 4 – Oct 30
1LAC: 1 year catalog: 2008 Aug 4 – 2009 July 4

3EG (**EGRET**):
10 >10σ |b|>10° sources
66 >5σ blazars

LBAS: subset of 0FGL w/ 205 sources
TS >100 (>10σ)
106 |b|>10° sources
assc. w/ AGNs

1FGL TS >25
1451 sources
1043 |b|>10° sources

1LAC
TS >25 (> 4.1σ)
671 assc. w/ 709 AGN
(663 hi-conf. associations)
(300 BL Lacs, 296 FSRQ, 41 other AGN, 72 unknown)

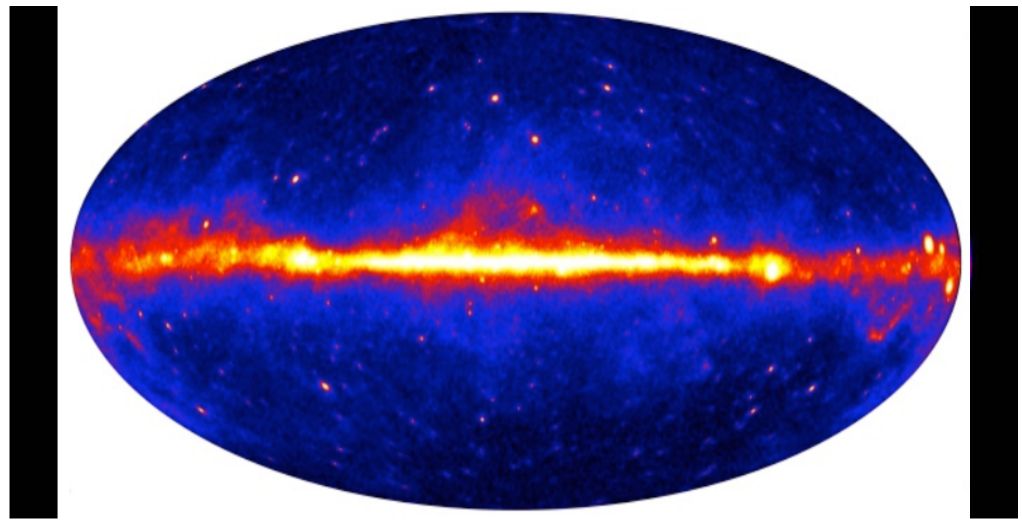

2 year Fermi GeV sky

2FGL TS >25
1888 sources — **832 AGNs (+268 candidates)**
114 Pulsars — **60 SNR/PWNe**
593 unaccounted — **7 others**

2LAC 360 FSRQs 420 BL Lacs (~60% with known z)
200 of unknown type ~20 other AGN

Classifying Fermi AGNs

Abdo et al. 2010, ApJ, 710, 1271

- **Radio:** FR1 vs FR2
- **Optical:** FSRQs vs. BL Lacs
- **SED;** ("synchrotron-peaked")

  LSP ($\nu_{pk}^{syn} < 10^{14}$ Hz),

  HSP ($\nu_{pk}^{syn} > 10^{15}$ Hz)

  ISP

Essentially all FSRQs are LSPs

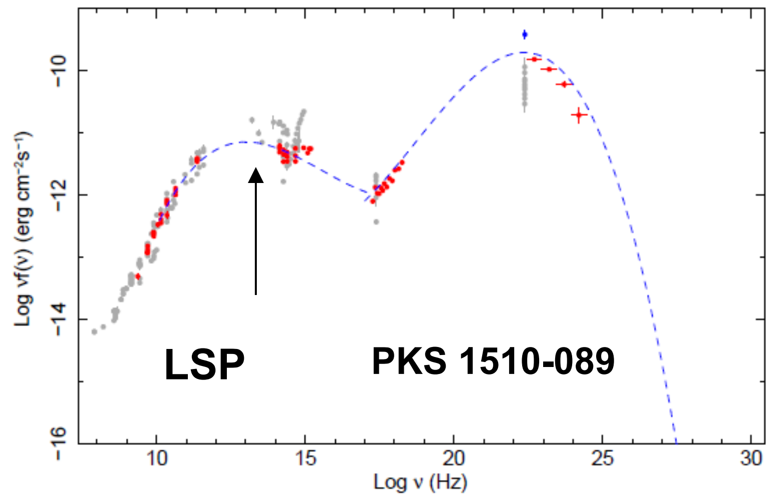

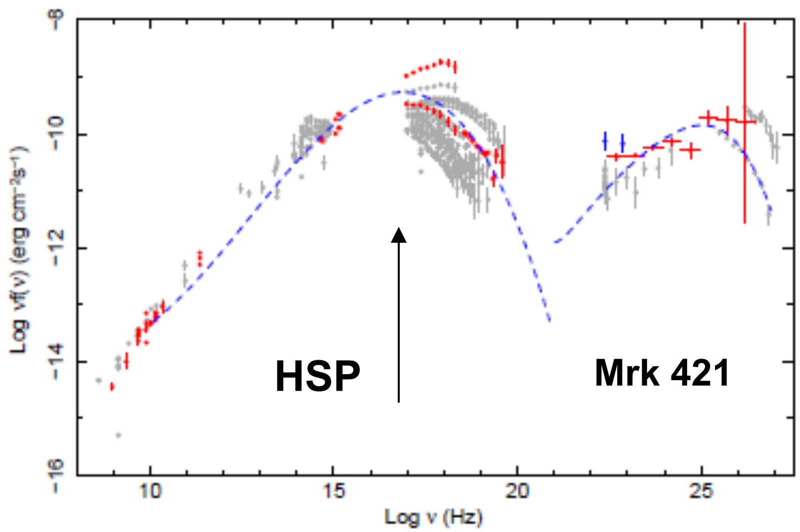

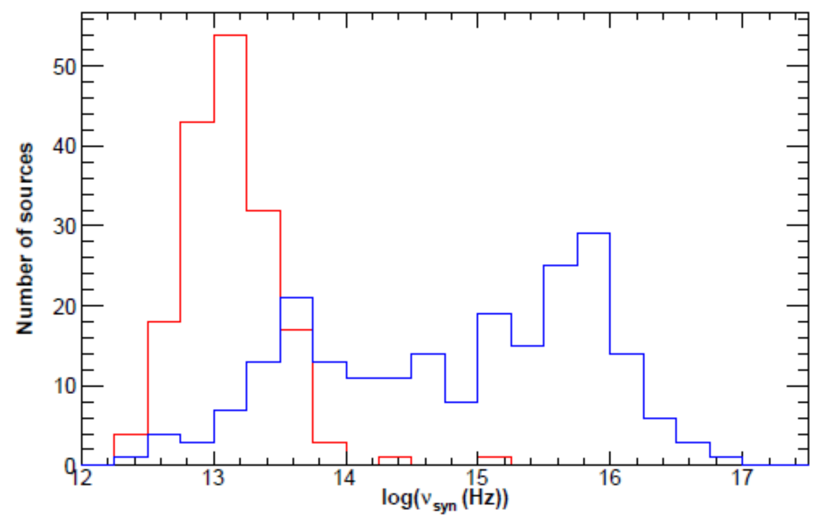

AGN Unification Paradigm

(Urry and Padovani 1995)

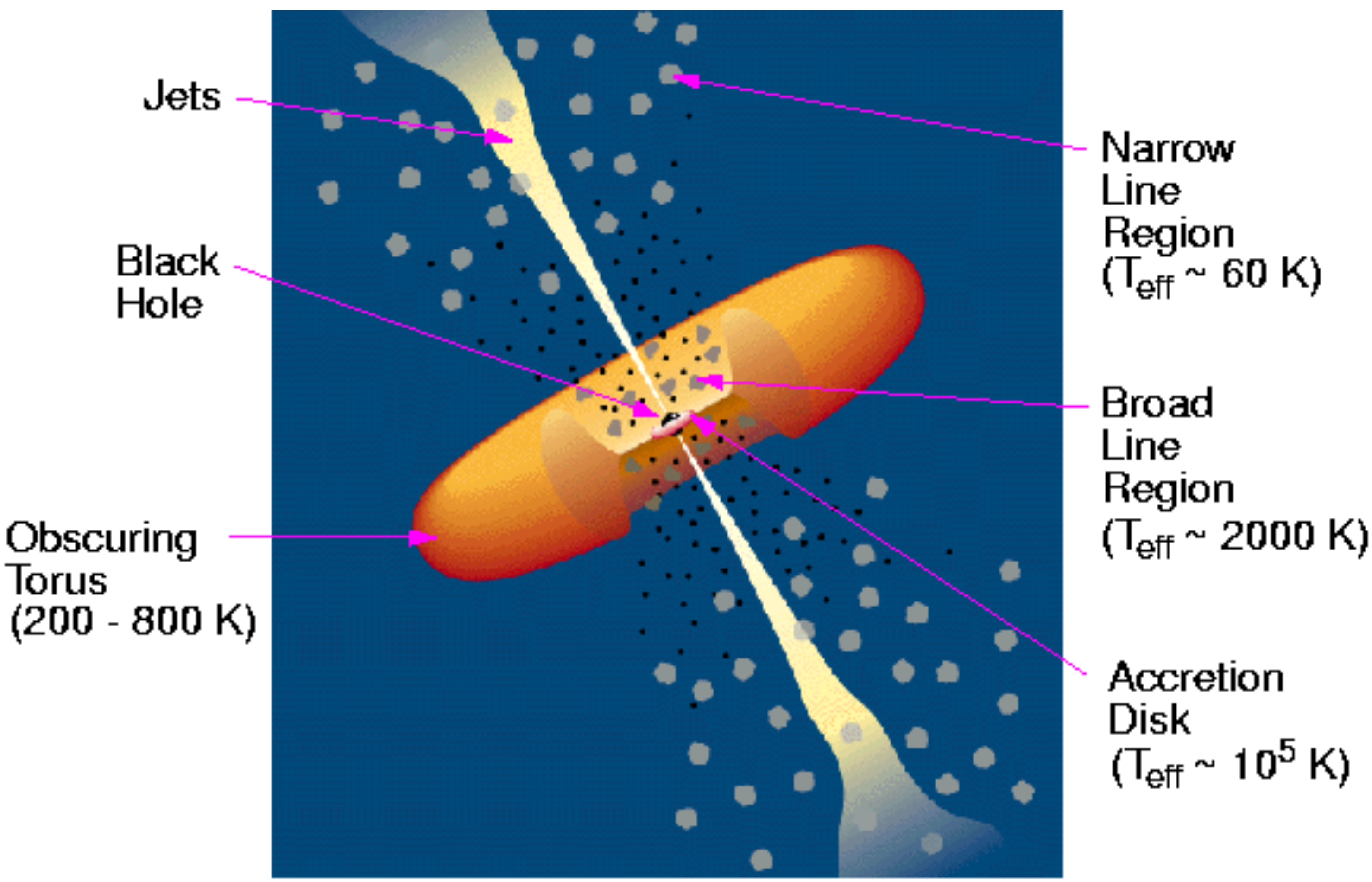

γ-Ray Galaxy Luminosity

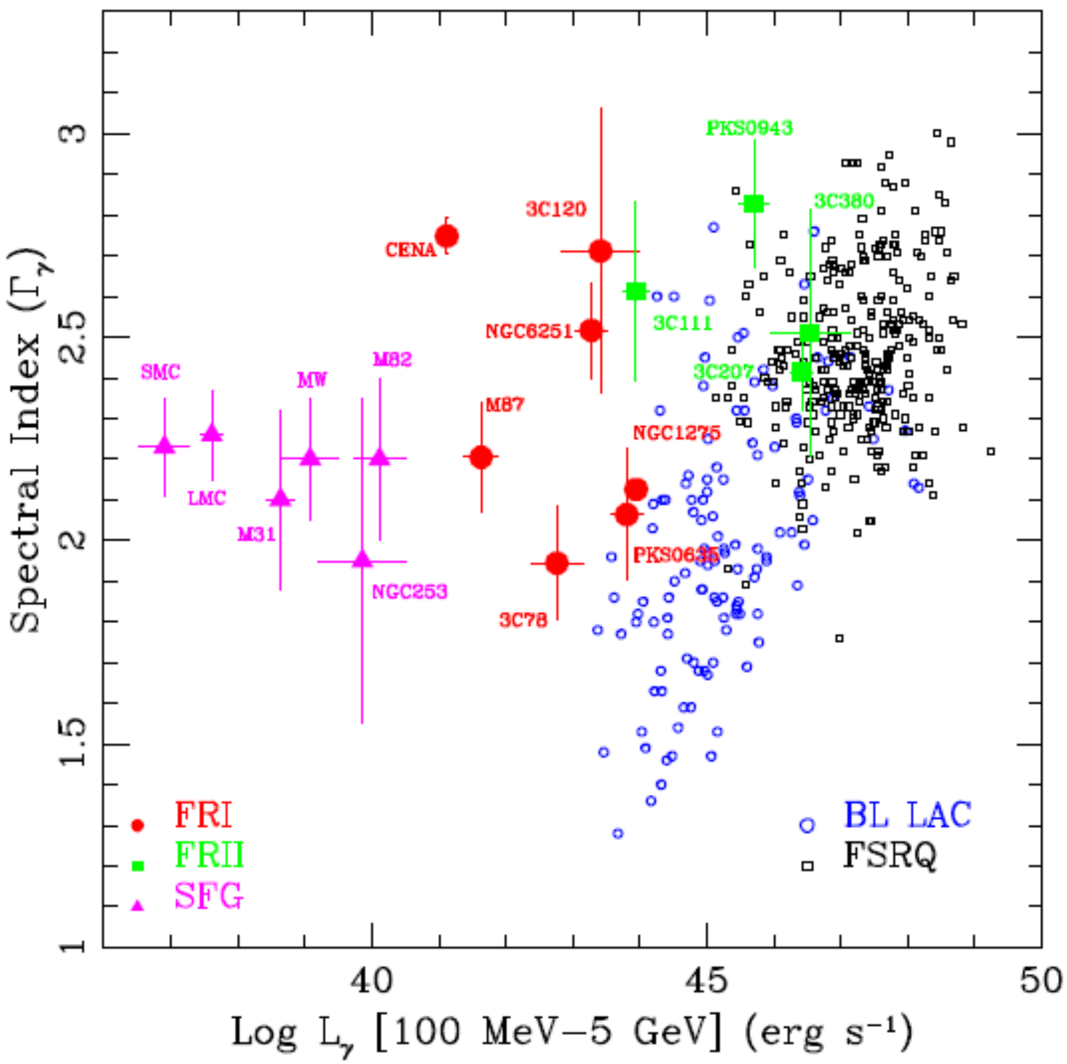

Fermi blazar divide
(Ghisellini et al. 2009)

Misaligned AGNs
(host galaxies of blazars)

Star forming galaxies

Spectral Index Distribution

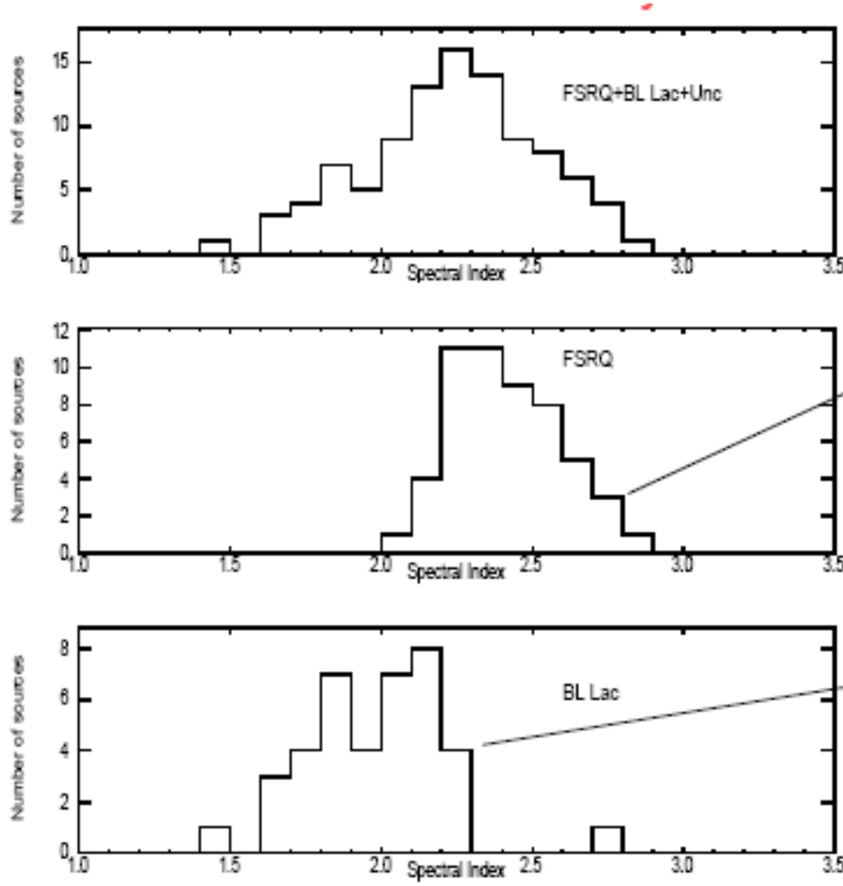

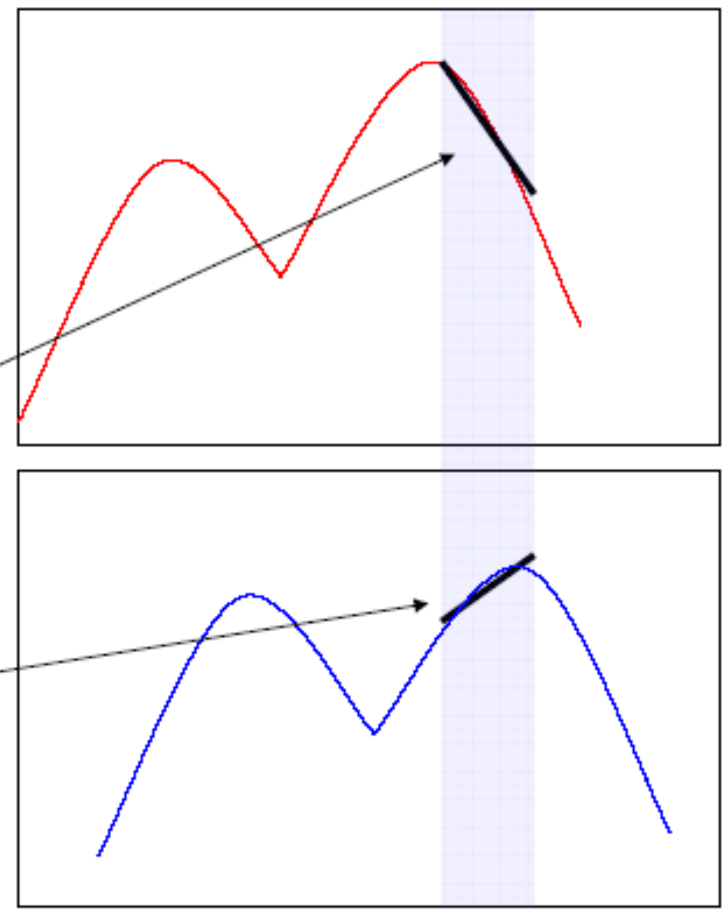

Blazar Sequence

- Searching for the Hertzsprung-Russell Diagram in blazar studies
- Inverse correlation between E_{peak} and luminosity
- Cooling model with external radiation for FSRQs (Ghisellini et al. 1998)
- Selection biases from 2 Jy FSRQs (Wall & Peacock catalog), 1 Jy BL Lac (radio selected), and Einstein Slew Survey (X-ray selected) (Giommi et al. 1999; Padovani et al. 2003, Padovani 2007)

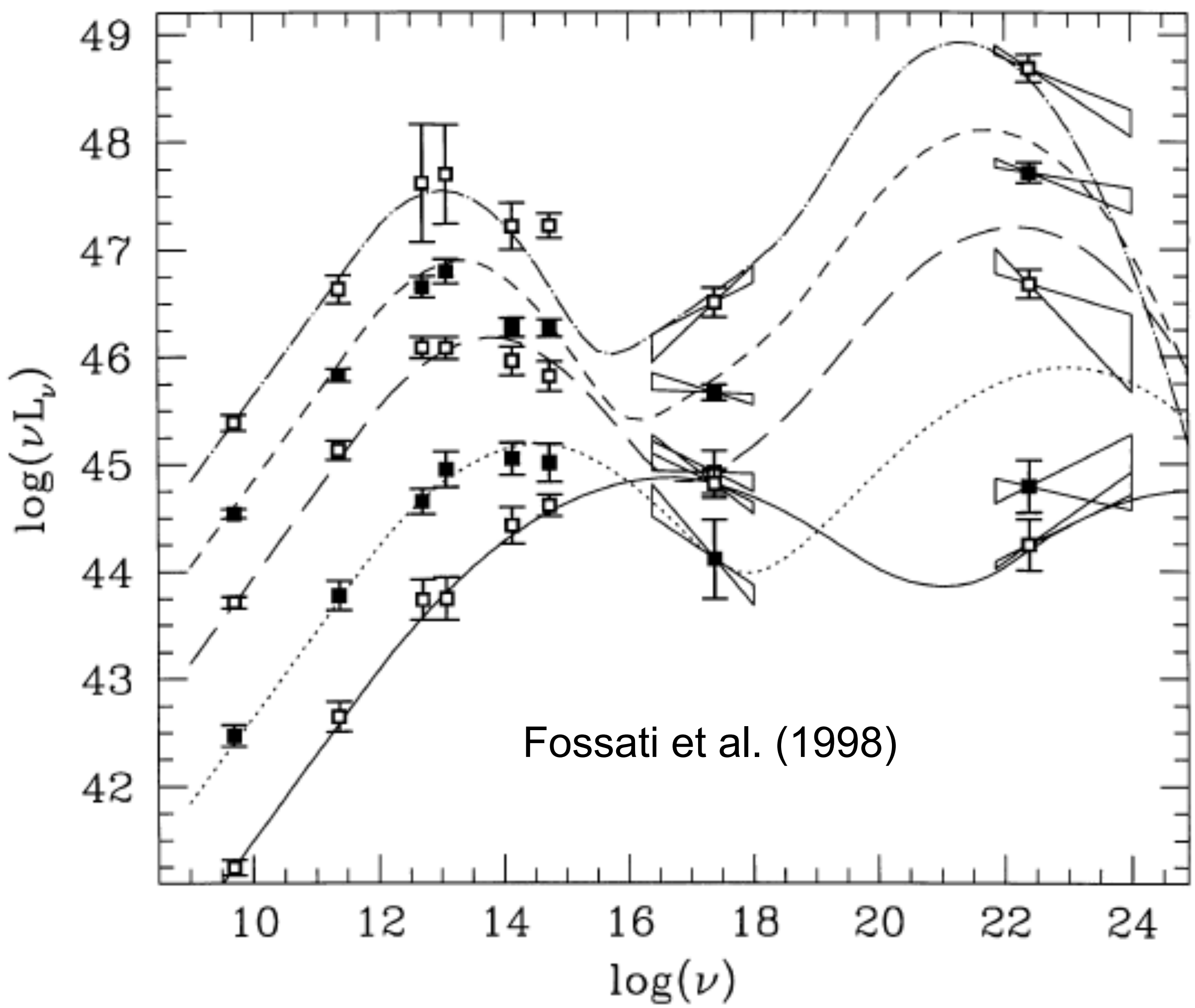

Understanding the Blazar Sequence

- **Inverse correlation between E_{peak} and luminosity** (Fossati et al. 1998)
- **Cooling model with external radiation for FSRQs** (Ghisellini et al. 1998)
- **Origin of the sequence**
  - **Galaxy evolution through reduction of fuel from surrounding gas and dust** (Böttcher and Dermer 2002)
  - **BZ effect** (Cavaliere and d'Elia 2002)

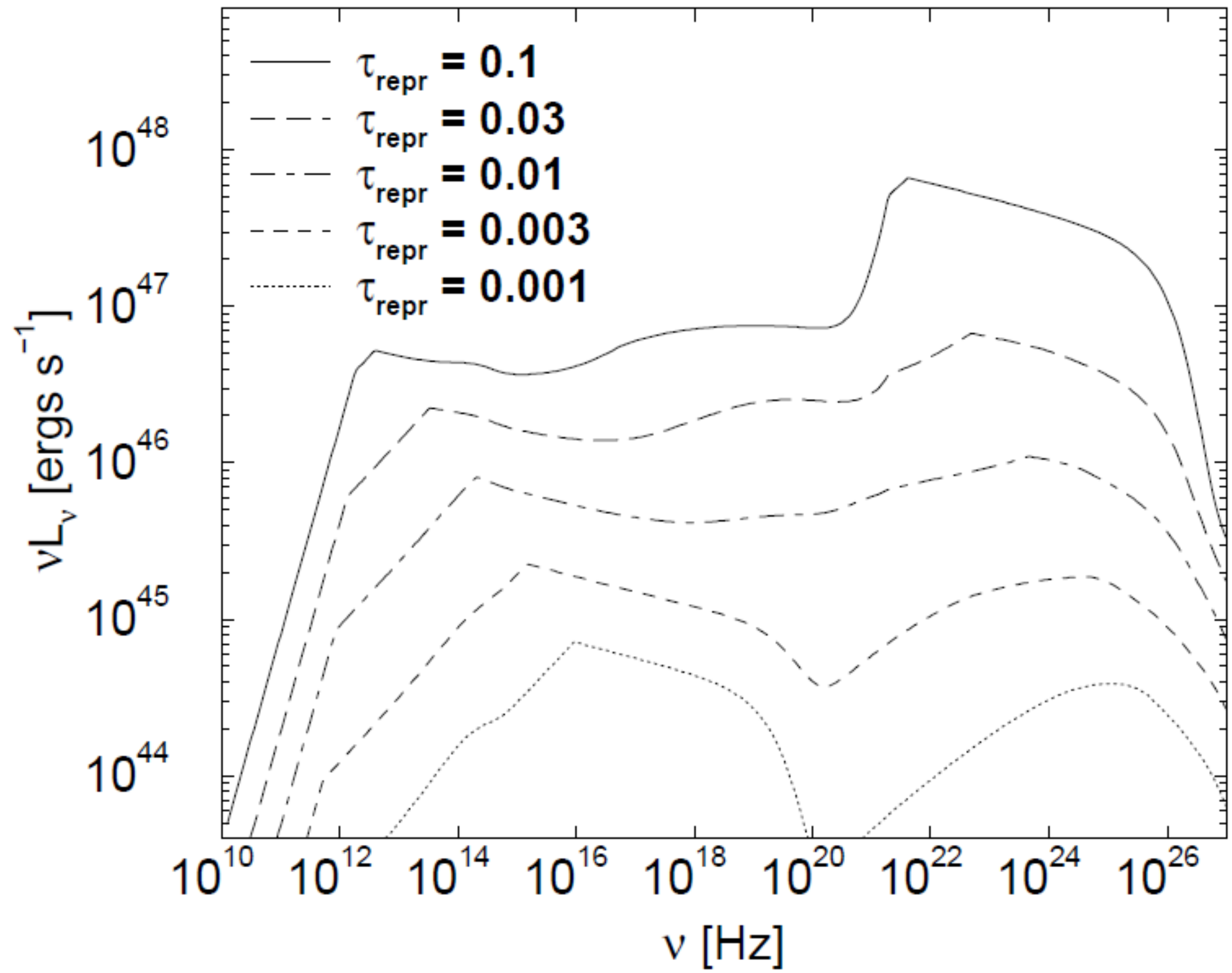

RLNL Sy 1s
PMN J0948+0022
z=0.585

Abdo et al. 2009, ApJ, 699, 976

Spectral Energy Distributions of Blazars: Two Component Paradigm

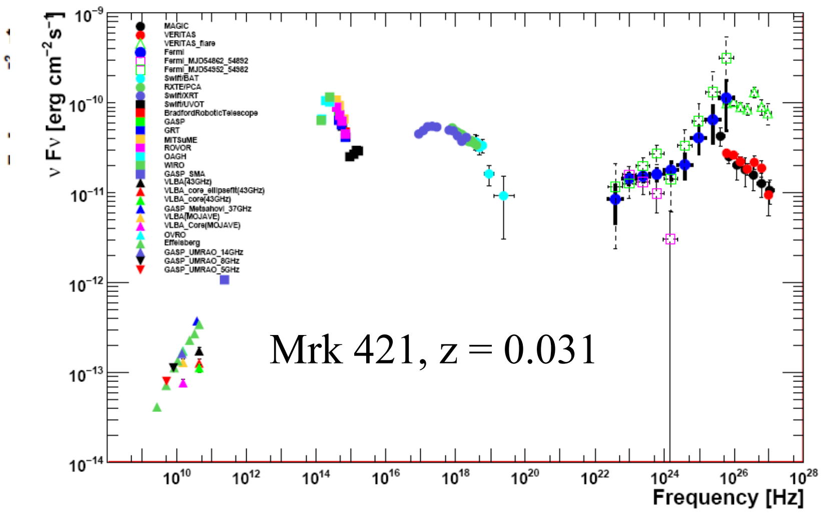

Abdo, et al. 2009, ApJ, 699, 817

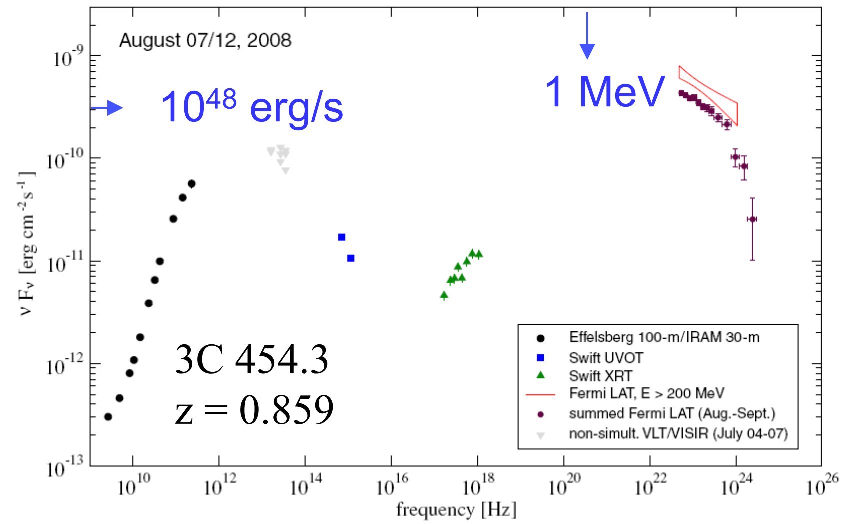

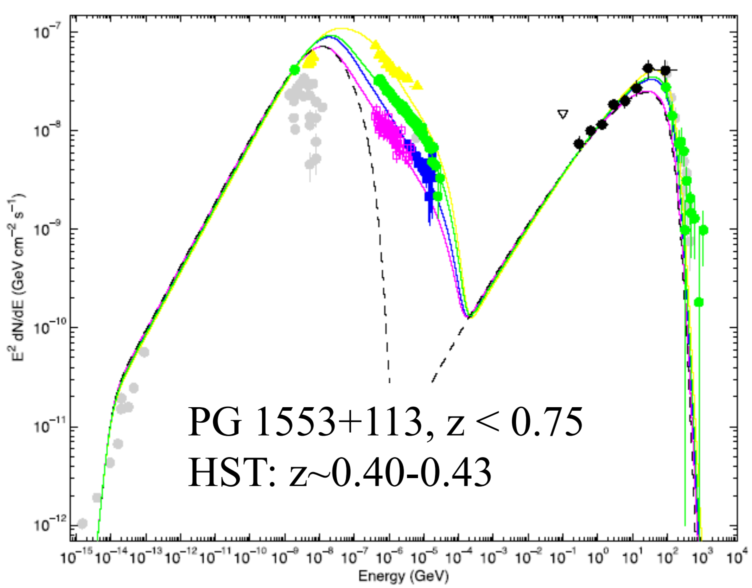

Abdo, et al. 2010, ApJ, 708, 1310

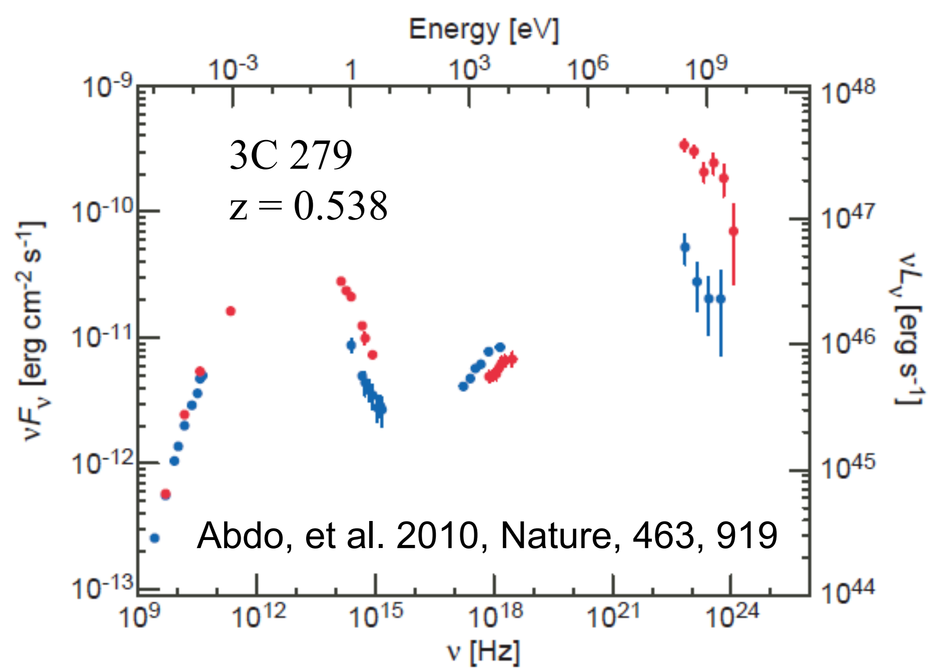

Blazar Modeling

Nonthermal γ rays $\Rightarrow$ relativistic particles + intense photon fields

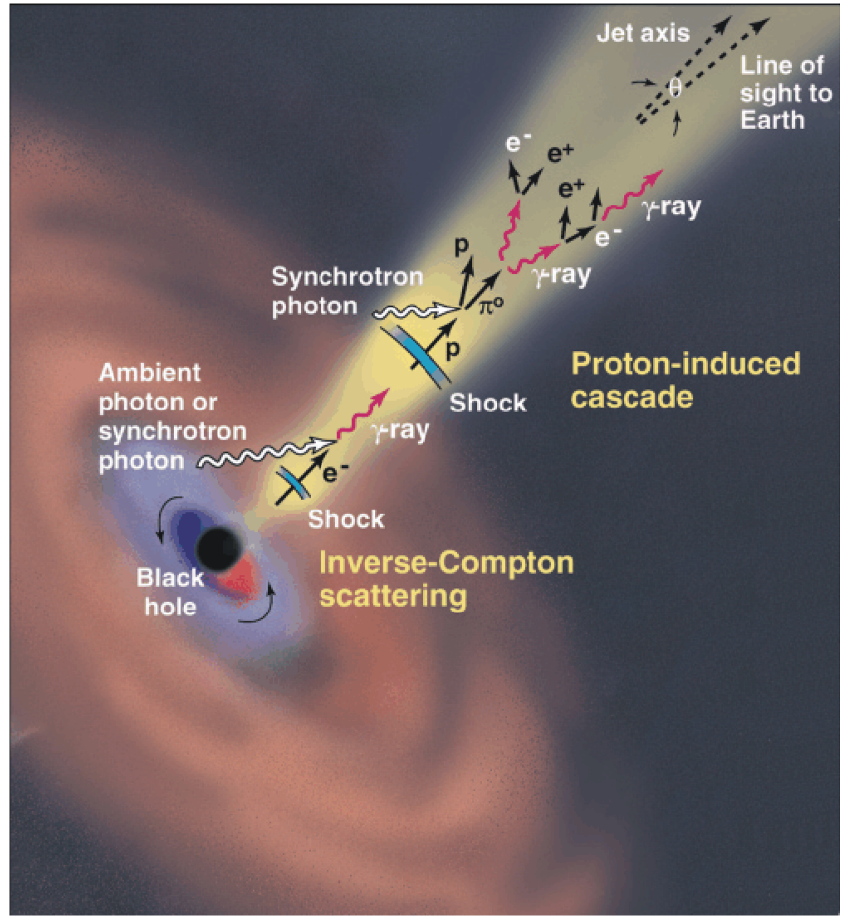

Leptonic jet model:

Nonthermal synchrotron paradigm
Associated SSC and EC component(s)
Location of emission site

Hadronic jet model:

Secondary nuclear production

$$pN \rightarrow \pi^o, \pi^\pm \rightarrow \gamma, \nu, n, e^\pm$$

Proton and ion synchrotron radiation

$$pB \rightarrow \gamma$$

Photomeson production

$$p\gamma \rightarrow \pi^o, \pi^\pm \rightarrow \gamma, \nu, n, e^\pm$$

High energy γ-ray component from $\gamma\gamma' \rightarrow e^\pm \rightarrow \gamma$ by Compton or synchrotron processes

Neutrons escape to become UHECRs

Black Hole Jet Physics: AGNs

Synchrotron/Compton
Leptonic Jet Model

BL Lac vs. FSRQs
Target photons for scattering
Accretion regime

Blob Formalism

Energy Sources:
1. Accretion Power
2. Rotation Power

Supermassive Black Holes

Identifying hadronic emissions

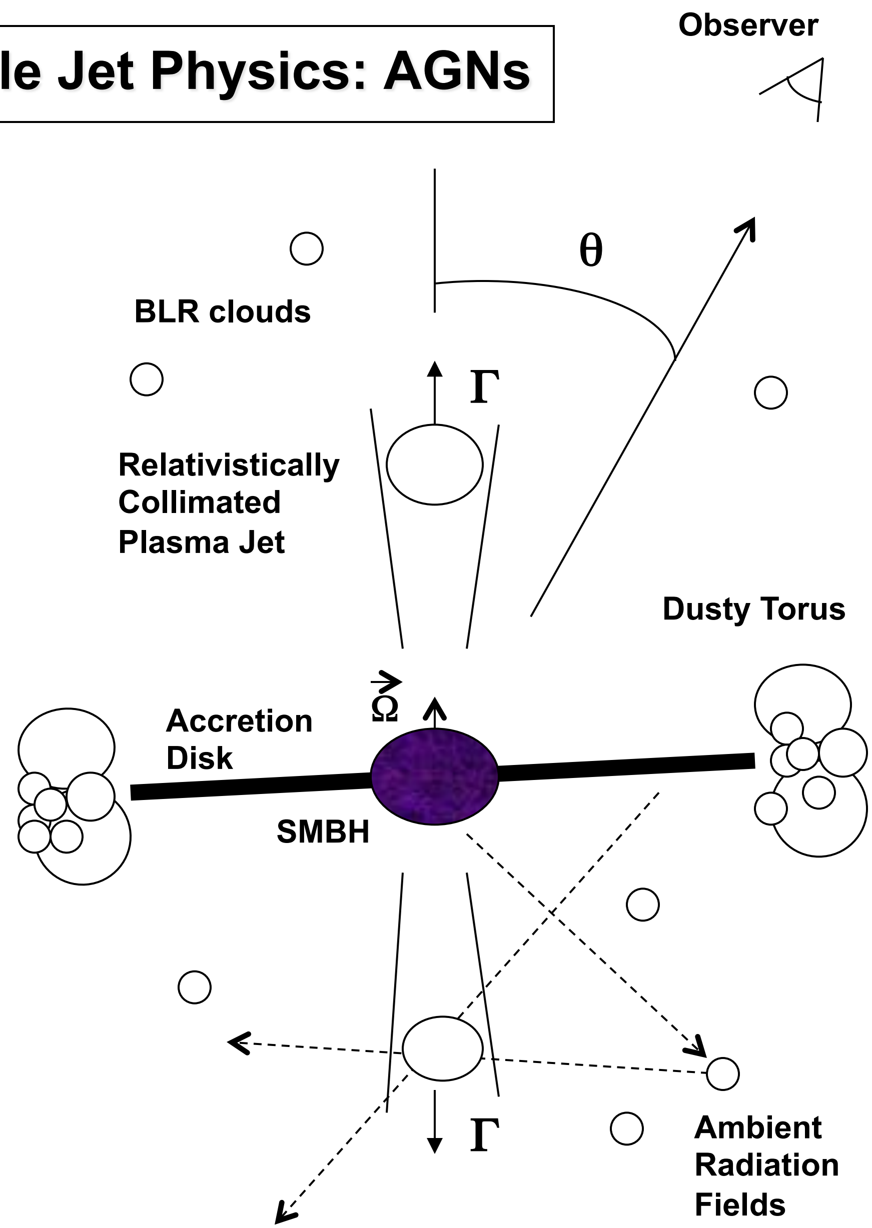

Doppler Factor

$$\delta_D \equiv [\Gamma(1-\beta\cos\theta)]^{-1}$$

$$\Delta x = \beta c \Delta t_* = \beta\Gamma c \Delta t'$$

$$t = t_* + \frac{d}{c} - \frac{x\cos\theta}{c}$$

$$t + \Delta t = t_* + \Delta t_* + \frac{d}{c} - \frac{(x+\Delta x)\cos\theta}{c}$$

$$\Rightarrow \Delta t = \frac{\Delta x}{\beta c}(1-\beta\cos\theta) = \Gamma\Delta t'(1-\beta\cos\theta)$$

$$\Rightarrow \Delta t = \frac{\Delta t'}{\delta_D}$$

$$\theta = 0 \Rightarrow \Delta t = \frac{\Delta x}{\beta c}(1-\beta) \to \frac{\Delta x}{\Gamma^2 c}$$

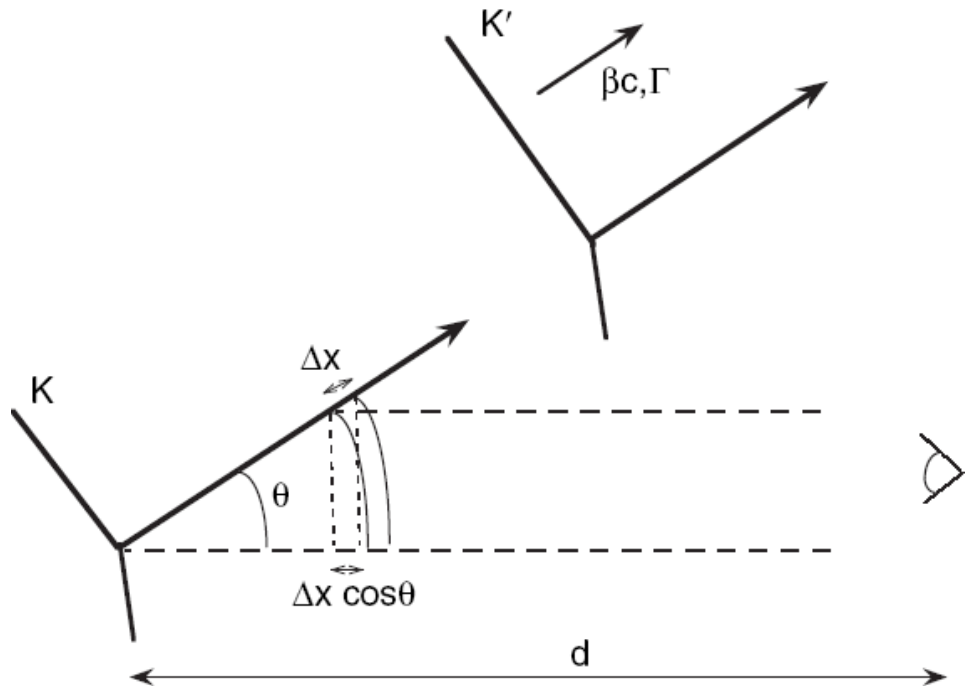

$$dt = \frac{(1+z)dt'}{\delta_D}$$

$$\varepsilon = \frac{\delta_D \varepsilon'}{(1+z)}$$

Variability and Source Size

Source size from direct observations:

$$r_b' \cong d_A\vartheta \cong 2\left(\frac{d_A}{10^{27}\,cm}\right)\vartheta(mas)\ pc$$

Source size from temporal variability:

$$r_b' \lesssim ct_{var}' = c\delta_{\rm D} t_{var}/(1+z)$$

$$r_b'(cm) < \frac{2.5\times 10^{15}\,\delta_D t_{\rm var}(day)}{(1+z)}$$

Spherical blob in comoving frame

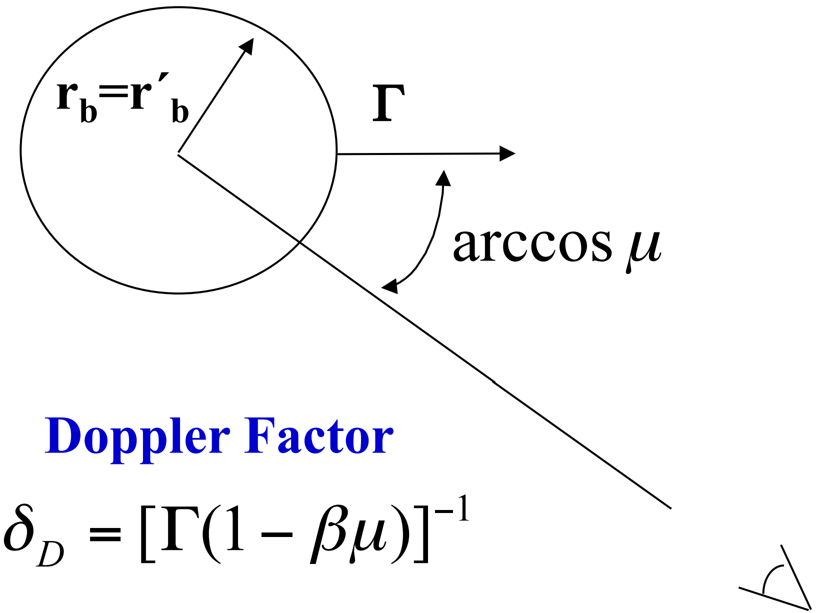

Doppler Factor

$$\delta_D = [\Gamma(1-\beta\mu)]^{-1}$$

Variability timescale implies maximum emission region size scale

Variability and Source Location

$$c\Delta t/(1+z) \cong x(1-\cos\theta) \cong x\theta^2/2 \cong x/2\Gamma^2$$
$$\Rightarrow x \cong 2\Gamma^2 c\Delta t/(1+z)$$

$$R_S = \frac{2GM}{c^2} < \frac{ct_{\rm var}}{(1+z)}$$

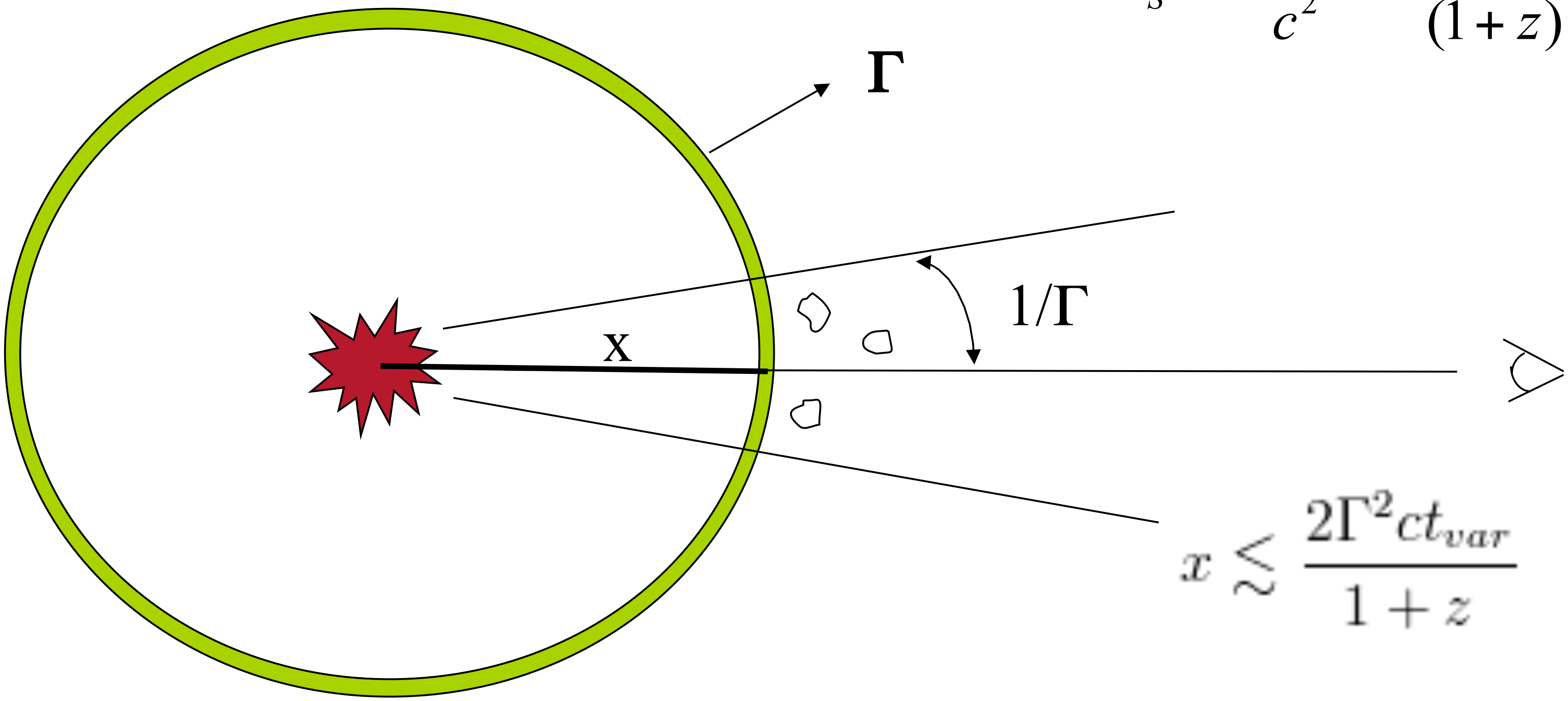

$$x \lesssim \frac{2\Gamma^2 ct_{var}}{1+z}$$

Variability timescale implies engine size scale, comoving size scale factor ≈Γ larger and emission location ~Γ^2 larger than values inferred for stationary region

Rapid variability by energizing regions within the Doppler cone

Energy Fluxes, Blobs and Blast Waves

Measured: **z** (⇒ d_L), **νF_ν** flux, **t_v** and jet angle **θ_j** for blob model

Total Energy Flux: $$\Phi = \frac{dE}{dAdt} = \frac{L}{4\pi d_L^2}$$

Spectral Energy Flux:

$$f_\varepsilon (erg\ cm^{-2}\ s^{-1}) = \nu F_\nu$$

$$Blob : \Phi \approx \delta_D^4 \frac{L'_\gamma}{4\pi d_L^2}$$

$$f_\varepsilon = \nu F_\nu = \frac{\delta_D^4 \varepsilon' L'(\varepsilon')}{4\pi d_L^2}, r'_b = \frac{c\delta_D t_v}{1+z}$$

$$Blast\ Wave : \Phi \approx \Gamma^2 \frac{L'_\gamma}{4\pi d_L^2}$$

$$f_\varepsilon = \nu F_\nu = \frac{\Gamma^2 \varepsilon' L'(\varepsilon')}{4\pi d_L^2}, R = \frac{c\Gamma^2 t_v}{1+z}, R' = R/\Gamma$$

Blob (off-axis jet model) vs. Blast Wave (observer within jet cone)

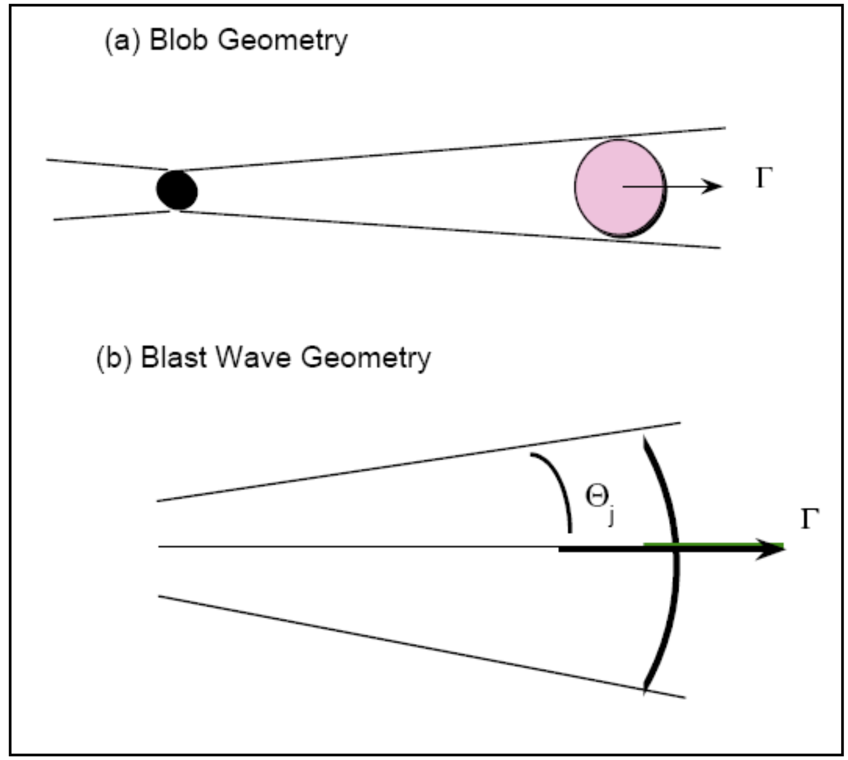

Blob and blast wave framework are equivalent for opacity calculations

Internal Radiation Fields

Instantaneous energy flux Φ (erg cm^{-2} s^{-1}); variability time t_v, redshift z

Blob:

$$\Phi \approx \delta_D^4 \frac{L'_\gamma}{4\pi d_L^2}, \quad u'_\gamma \sim \frac{L'_\gamma t'_{esc}}{V'} \sim \frac{3 d_L^2 \Phi}{\delta_D^4 r'^2 c}, \quad t'_{esc} \sim r'/c \sim \Delta t' \approx \frac{\delta_D t_v}{1+z}$$

$$u'_\gamma \approx \frac{3 d_L^2 (1+z)^2 \Phi}{\delta_D^6 t_v^2 c^3} \qquad or \quad n'_\gamma(\varepsilon') \cong \frac{3 d_L^2 (1+z)^2 f_\varepsilon}{m_e c^5 \varepsilon'^2 \delta_D^6 t_v^2}$$

$$n'_{ph}(\varepsilon') \cong \frac{3 d_L^2 f_\varepsilon}{m_e c^3 \varepsilon'^2 \delta_D^4 r'^2} \qquad r' \approx \frac{c \delta_D t_v}{1+z}, \quad \varepsilon' \cong \frac{(1+z)\varepsilon}{\delta_D}$$

Blast Wave:

$$u'_\gamma \cong \frac{4\pi d_L^2 \Phi}{4\pi R^2 \Gamma^2 c} \cong \frac{d_L^2 (1+z)^2 \Phi}{\Gamma^6 t_v^2 c^3} \quad or \quad n'_\gamma(\varepsilon') \cong \frac{d_L^2 (1+z)^2 f_\varepsilon}{m_e c^5 \varepsilon'^2 \Gamma^6 t_v^2}$$

$$R' = R/\Gamma, R = \frac{c \Gamma^2 t_v}{1+z}, \quad \varepsilon' \cong \frac{(1+z)\varepsilon}{\Gamma}$$

Internal Magnetic Fields and Power

Internal energy density $u' = u'_\gamma/\varepsilon_e$ implies a jet magnetic field

$$B' \cong \sqrt{8\pi \varepsilon_B u'_\gamma / \varepsilon_e}$$

ε_e is fraction of total energy density in nonthermal electrons assumed to be producing the γ rays

ε_B is fraction of total energy density in magnetic field

Apparent Jet Power

$$P_j = 4\pi R^2 \beta c \Gamma^2 (u'_B + u'_{par} + u'_\gamma)$$

Absolute Jet Power

$$r'_b \approx \frac{c\delta_D t_v}{1+z}$$

$$P_j = 2\pi r_b'^2 \beta c \delta_D^2 \left(\frac{\Gamma^2}{\delta_D^2}\right)(u'_B + u'_{par} + u'_\gamma)$$

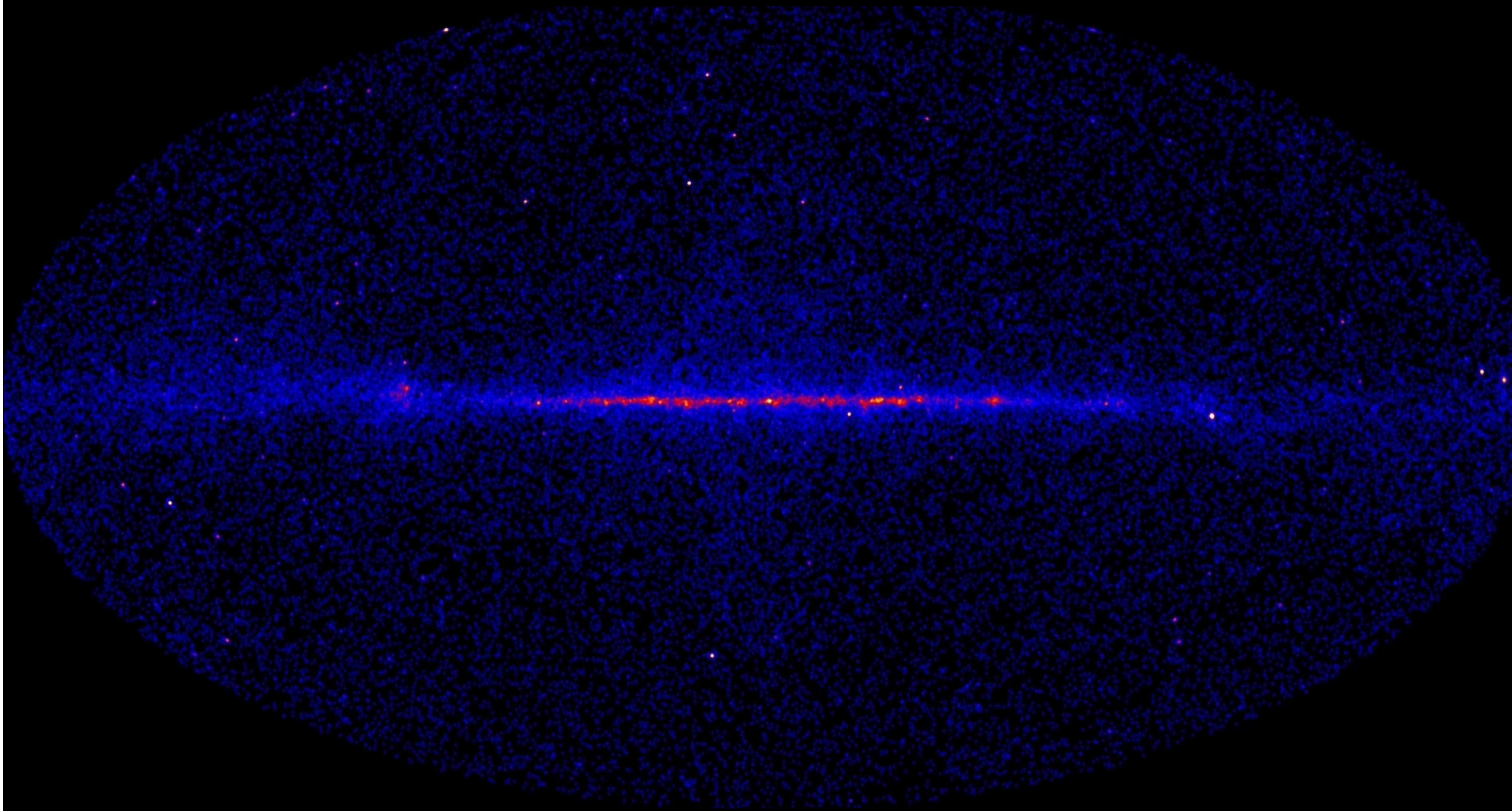

3 month Fermi LAT data

>200 MeV

1 Year Fermi LAT data

10-100 GeV

γγ Opacity : δ-function approximation for Blob

$$\frac{d\tau_{\gamma\gamma}(\varepsilon_1')}{dx'} \cong \int_0^\infty d\varepsilon'\,\sigma_{\gamma\gamma}(s')n_{ph}'(\varepsilon'), \quad \sigma_{\gamma\gamma}(s') \cong \frac{2}{3}\sigma_T\delta(s'-2)$$

$$\tau_{\gamma\gamma}(\varepsilon_1') \approx \frac{2}{3}\sigma_T r'\int_0^\infty d\varepsilon'\,\frac{\delta(\varepsilon'-2/\varepsilon_1')}{\varepsilon_1'}n_{ph}'(\varepsilon') \qquad \varepsilon' = 2/\varepsilon_1'$$

$$\approx \frac{2}{3}\frac{\sigma_T r' n_{ph}'(2/\varepsilon_1')}{\varepsilon_1'} \qquad n_\gamma'(\varepsilon') \cong \frac{3d_L^2(1+z)^2 f_\varepsilon}{m_e c^5 \varepsilon'^2 \delta_D^6 t_v^2}$$

$$n_{ph}'(\varepsilon') \cong \frac{3d_L^2 f_\varepsilon}{m_e c^3 \varepsilon'^2 \delta_D^4 r'^2} \qquad \Rightarrow \tau_{\gamma\gamma}(\varepsilon_1') \cong \frac{2\sigma_T}{3\varepsilon_1'}\frac{3d_L^2 f_\varepsilon}{m_e c^3 \varepsilon'^2 \delta_D^4 r'}$$

$$\varepsilon' = \frac{(1+z)\varepsilon}{\delta_D}$$

Minimum Doppler factor approximation for Blob

$$\tau_{\gamma\gamma}(\varepsilon_1') \cong \frac{2\sigma_T}{\varepsilon_1'} \frac{d_L^2 f_\varepsilon}{m_e c^3 \varepsilon'^2 \delta_D^4 r'}$$

$$\tau_{\gamma\gamma}(\varepsilon_1') \cong \frac{\sigma_T}{2} \frac{d_L^2 f_\varepsilon \varepsilon_1'}{m_e c^3 \delta_D^4 r'}$$

$$\tau_{\gamma\gamma}(\varepsilon_1) \cong \frac{\sigma_T (1+z)^2 d_L^2 f_{\hat{\varepsilon}} \varepsilon_1}{2 m_e c^4 \delta_D^6 t_v}$$

$$\varepsilon' = 2/\varepsilon_1'$$

$$\varepsilon_1' = \frac{(1+z)\varepsilon_1}{\delta_D}$$

$$r' \approx \frac{c\delta_D t_v}{1+z},$$

Minimum bulk Lorentz factor: $\tau_{\gamma\gamma}(\varepsilon_1) = 1$

$$\Rightarrow \delta_{D,\min} \cong \left[\frac{\sigma_T (1+z)^2 d_L^2 f_{\hat{\varepsilon}} \varepsilon_1}{2 m_e c^4 t_v}\right]^{1/6}$$

$$\varepsilon' \varepsilon_1' \approx 2 \Rightarrow \hat{\varepsilon} \cong \frac{2\delta_D^2}{(1+z)^2 \varepsilon_1}$$

γγ opacity and Γ_{min} for PKS 2155-304

$$\delta_{D,\min} \cong \left[\frac{\sigma_T (1+z)^2 d_L^2 f_{\hat{\varepsilon}} \varepsilon_1}{2 m_e c^4 t_v}\right]^{1/6}$$

$$\hat{\varepsilon} \cong \frac{2\delta_D^2}{(1+z)^2 \varepsilon_1}$$

z = 0.116, d_L = 1.65×10^{27} cm

t_v= 300 t_{5m} s

Solve iteratively, quickly converges

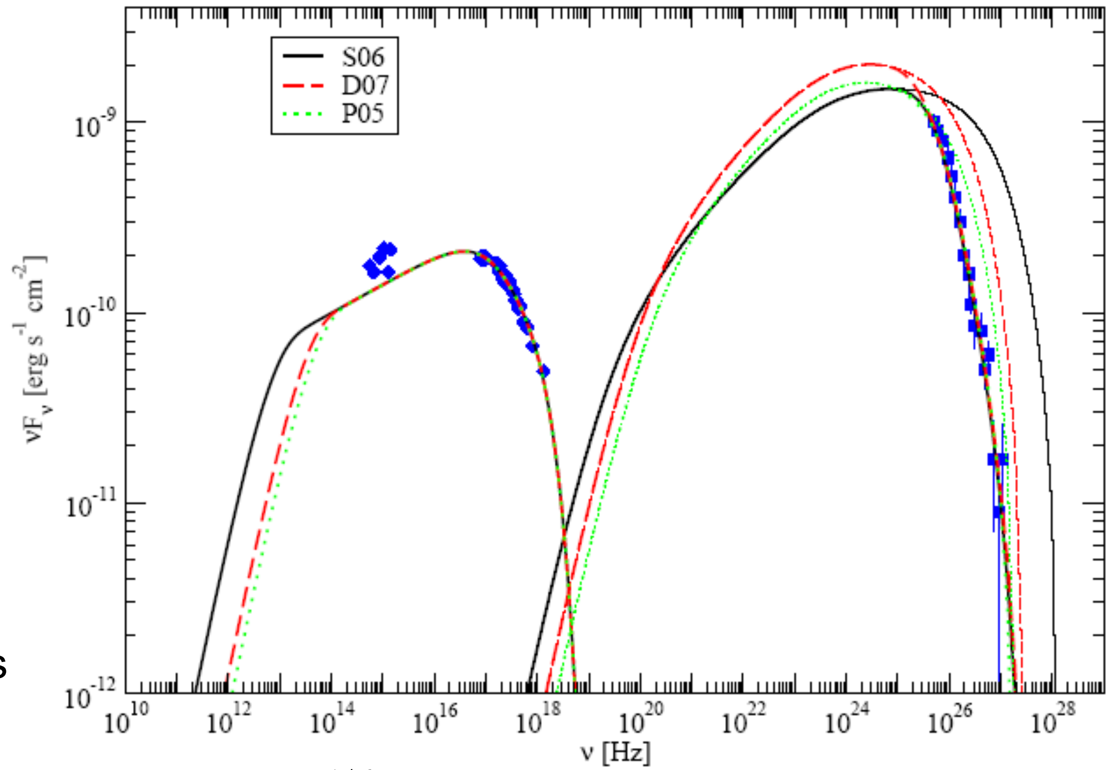

$$\delta_{D,\min} \cong 32\left[\frac{(f_{\hat{\varepsilon}}/10^{-10}\, erg\ s^{-1} cm^{-2}) E_1(TeV)}{t_{5m}}\right]^{1/6}$$

$$\widehat{E}(keV) \cong 0.6 \frac{(\delta_D/36)^2}{E_1(TeV)}$$

- Code of Finke et al. (2008)
- Includes internal γγ opacity but not pair reinjection
- Sensitive to EBL model
- Fit to 2006 flare

Synchrotron Self-Compton Model

Basic tool is one-zone synchrotron/SSC model with synchrotron self-absorption and internal pair production

Even this lacks pair reinjection; multiple self-Compton components

Deducing source redshift from high-energy spectra requires both good spectral model and good EBL model

What portion of synchrotron spectrum should be fitted?

Synchrotron/SSC model: Best fit model; parameter studies; extracting underlying electron distribution; variability analysis

Synchrotron/SSC Modeling

Approximations (in the one-zone model)

1. δ-function approximation
   - zero-fold for synchrotron; 1 fold for SSC
   - Take KN effects into account by terminating integration when scattering enters the KN regime
   - Useful for analytic results; equipartition estimates; jet power calculations

2. Uniform approximation: B, δ_D, and R'
   - a. Integrate elementary synchrotron emissivity over electron γ-factor distribution (assumed uniform throughout sphere)
   - b. Average synchrotron spectrum over blob to get target photon spectrum
   - c. Compton-scatter synchrotron photons using (isotropic) Jones formula, valid throughout Thomson and KN regimes
   - Provides accurate absolute power estimates (photon, particle, B-field) given observing angle
     for blazars, $\Gamma \approx \delta_D$; for radio galaxies inferred from observations

Synchrotron Self-Compton Modeling

Determine electron distribution from nonthermal synchrotron spectrum

Integrate electron spectrum over Crusius-Schlickeiser (1986) function to get accurate synchrotron emissivity;
See Finke et al. (2008)

Compton kernel in head-on approximation for SSC (Finke et al. 2008; Dermer et al. 2008

Spatially-averaged emission

Synchrotron self-absorption for homogeneous sphere

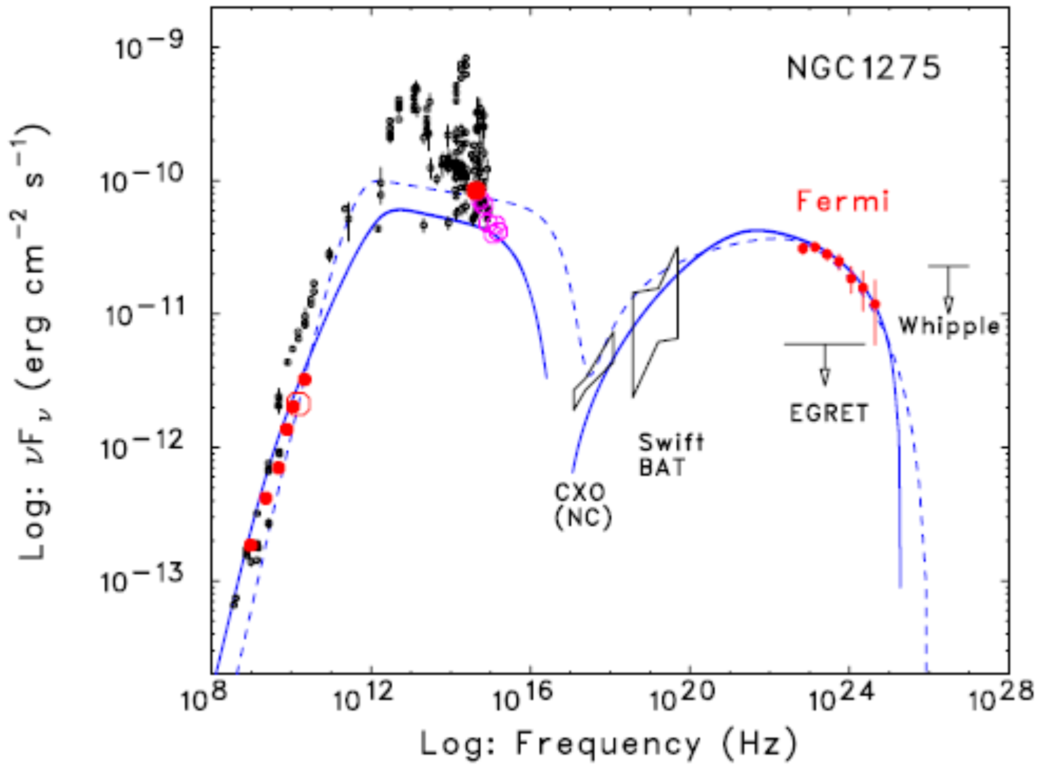

$$f_\varepsilon^{syn} \cong f_{\varepsilon_s}\left[\left(\frac{\varepsilon}{\varepsilon_0}\right)^{4/3}\left(\frac{\varepsilon_0}{\varepsilon_s}\right)^{a} H(\varepsilon;\varepsilon_0,\varepsilon_s)+\left(\frac{\varepsilon}{\varepsilon_s}\right)^{a} H(\varepsilon;\varepsilon_0,\varepsilon_s)+\left(\frac{\varepsilon}{\varepsilon_s}\right)^{b} H(\varepsilon;\varepsilon_s,\infty)\right]$$

$\gamma\gamma$ opacity and Γ_{min} for PKS 2155-304

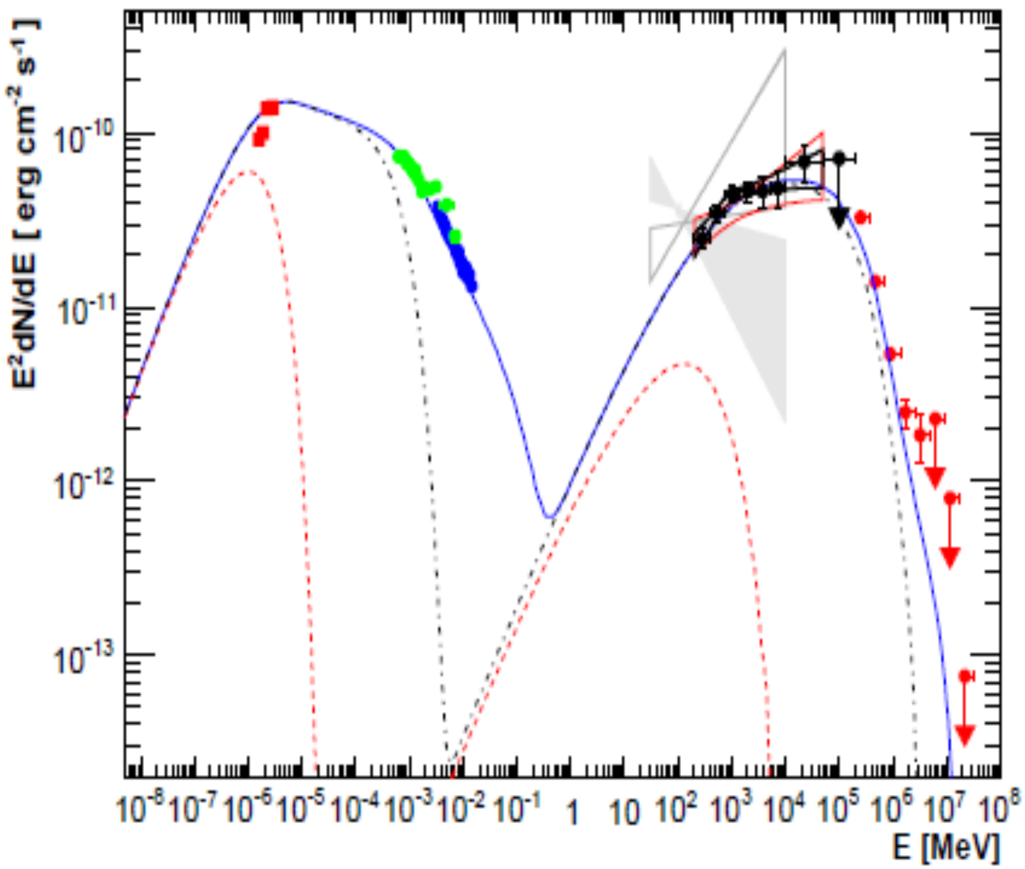

Model	δ_D	B [mG]	t_{var} [s]	L_j [10^{47} erg s^{-1}]
6	895	2.5	30	4.5
8	390	3.0	300	2.7
16	261	81	30	0.5
18	139	57	300	0.4

Lower EBL

Standard one-zone synchrotron/SSC model

$(\gamma'_{min} = 100)$

Doppler factor δ >> 100 during flaring episodes

- Radio galaxy core emission well fit by sync./SSC model with $\delta \approx \Gamma \approx$ few
- The δ-unification problem

-- Decelerating Jet Model

(Georganopoulos & Kazanas 2003)

-- Spine and Sheath Model

(Ghisellini et al. 2005)

-- Colliding Shell Model

NGC 6251: FR1 MAGN

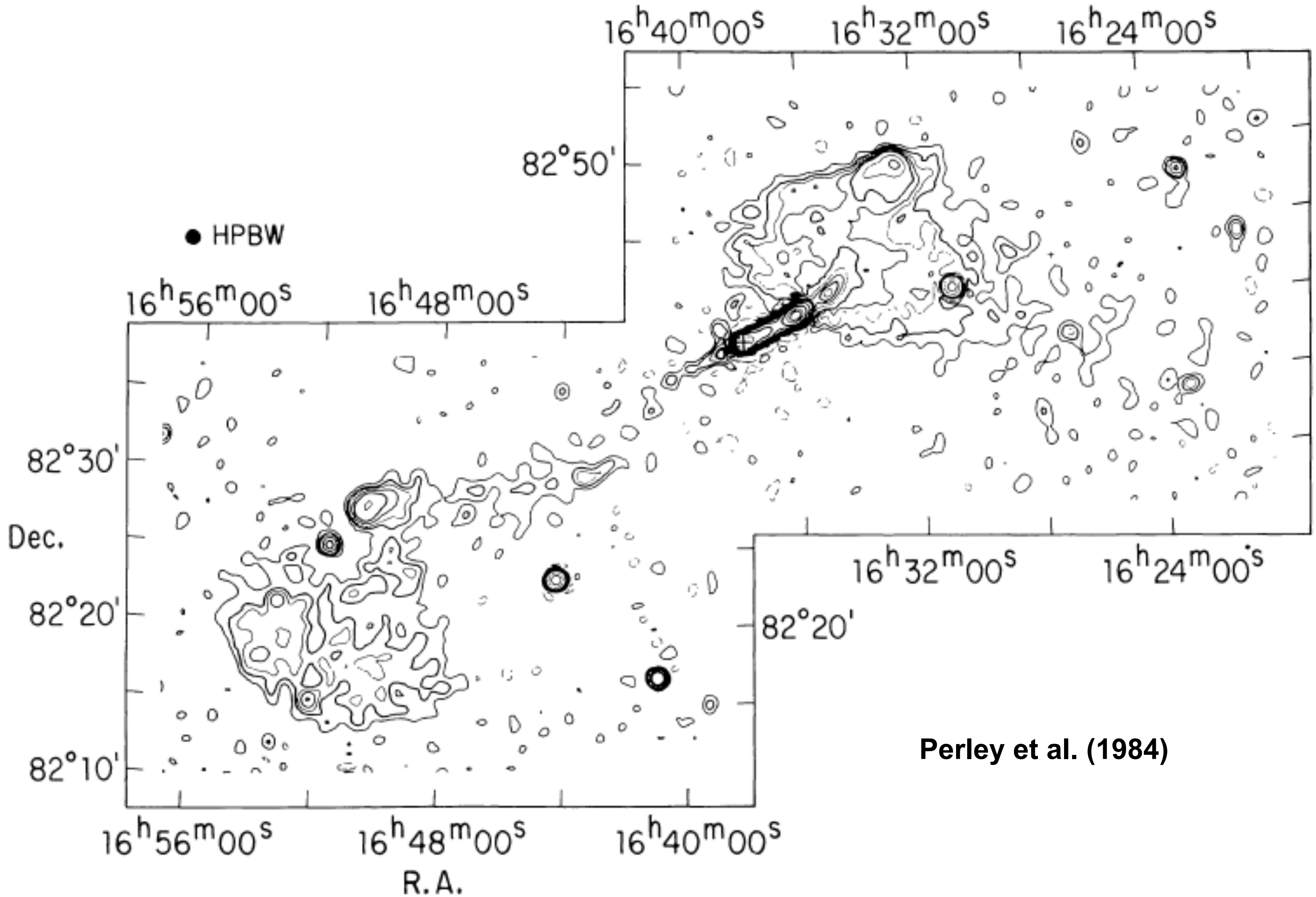

Perley et al. (1984)

Cen A Core and Lobes

- First resolved extragalactic GeV source (after LMC)

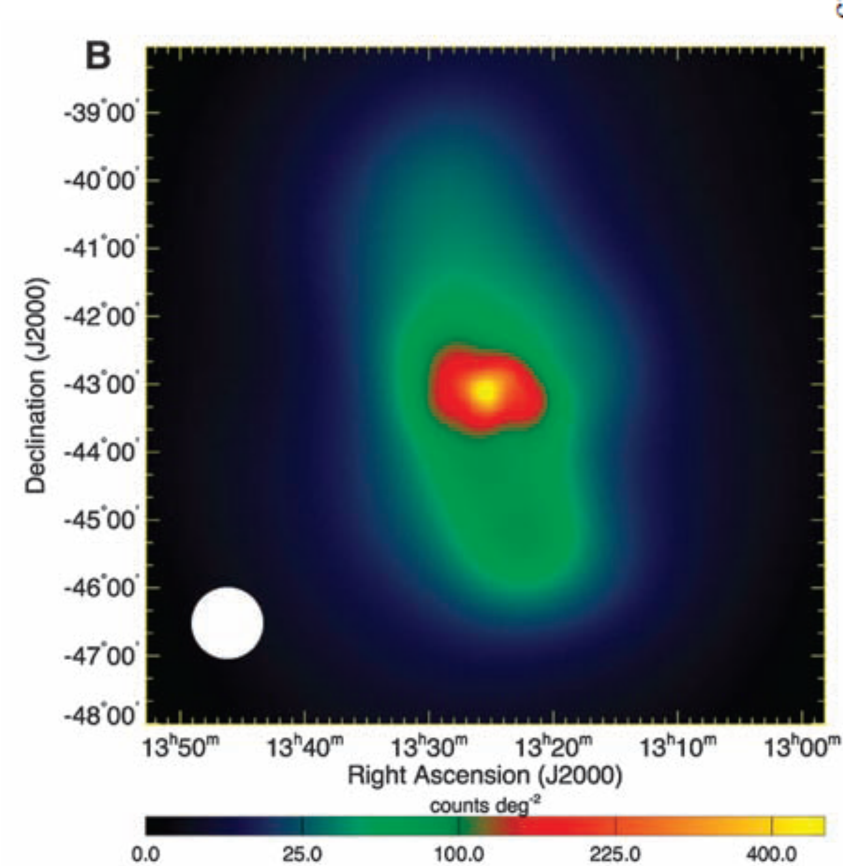

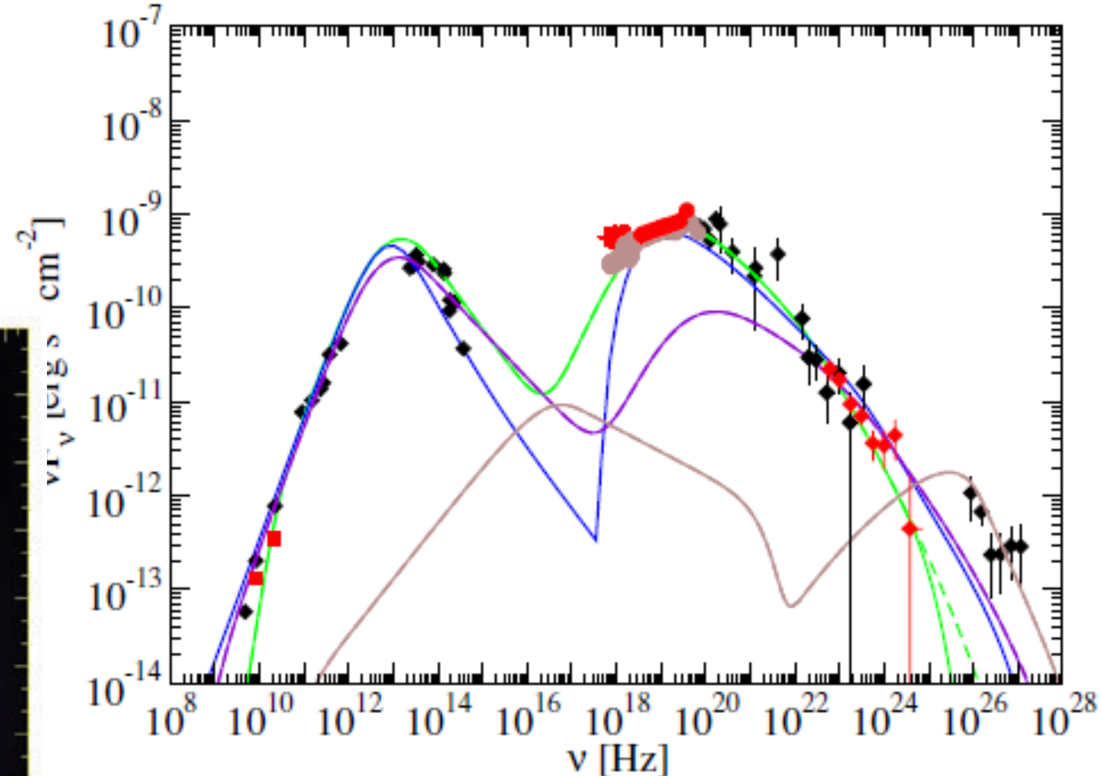

10 times more energy in nonthermal protons/hadrons as electrons

FSRQ Modeling

At least three additional spectral components:
- Accretion disk
- EC Disk
- EC BLR

External radiation field provides a new source of opacity; need to perform Compton scattering and γγ opacity self-consistently

Opacity spectral break at a few GeV

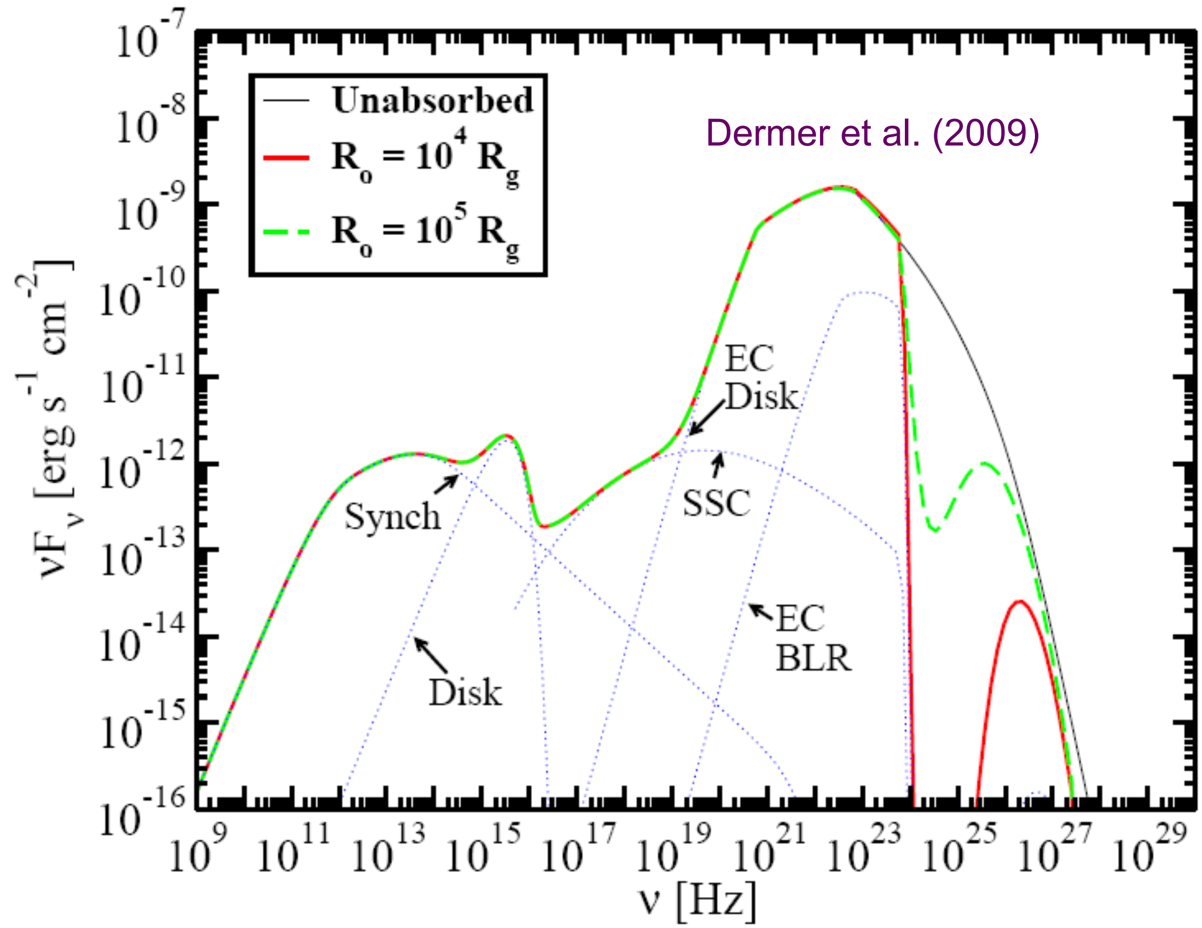

The Peculiarly Constant GeV Spectral Break in 3C 454.3

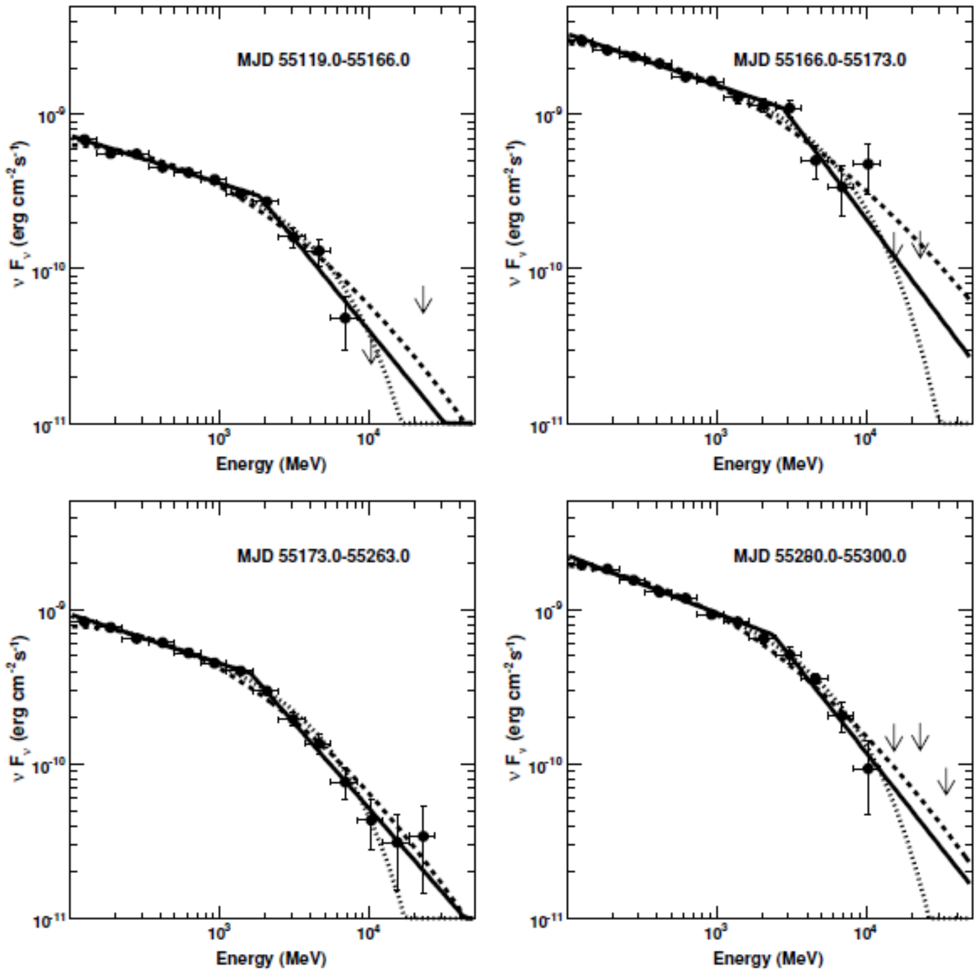

or ● MJD=55152-55261
● MJD=55280-55300

BPL, LogPar, Expcutoff

Γ_1	Γ_2	E_{break} (MeV)	α	β	Γ	E_b (MeV)	P (MeV)
$\pm$ 0.01	3.05$\pm$0.06	1590^{+190}_{-160}	2.51$\pm$0.02	0.13$\pm$0.01	2.29 $\pm$ 0.02	760$\pm$190	6000$\pm$600
$\pm$ 0.02	3.23$\pm$0.14	2380^{+750}_{-270}	2.55$\pm$0.03	0.10$\pm$0.02	2.35$\pm$0.03	960$\pm$500 MeV	7700$\pm$1500

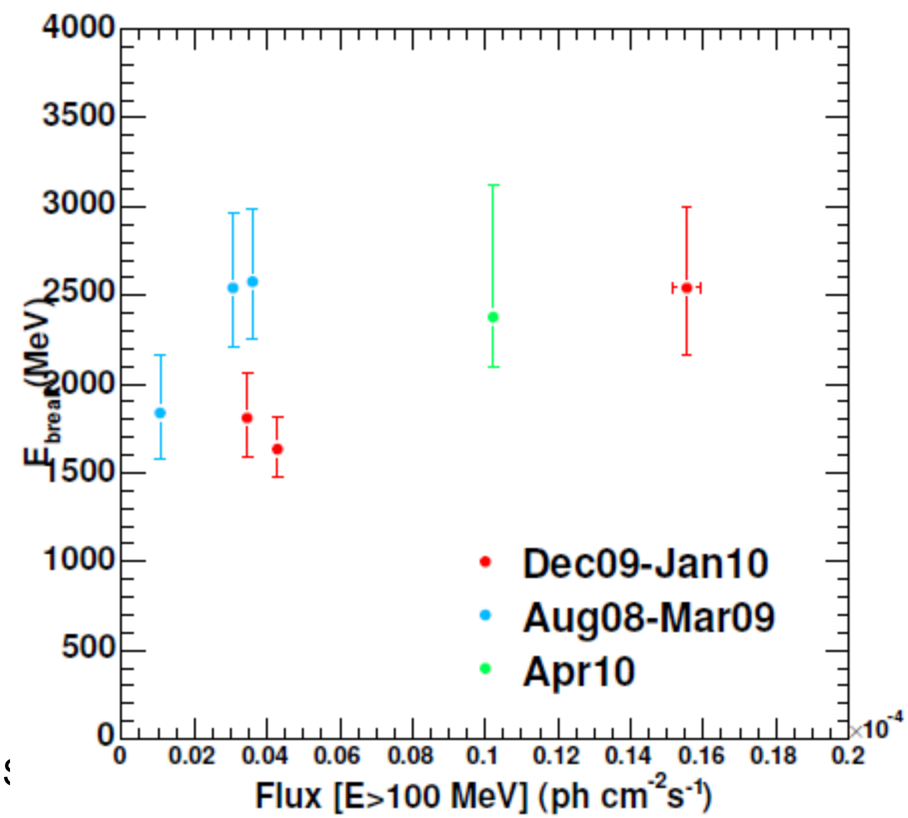

Dermer

Fermi Summer S

Models for Spectral Break

Intrinsic spectral break in electron energy distribution with Compton-scattered accretion disk and broad line region radiation (Finke & Dermer 2010)

Robust solution, independent of dissipation radius, within BLR with wind-density profile (disk-wind)

γγ attenuation from H (13.6 eV) and He II (54.4 eV) recombination radiation deep within the BLR (Poutanen & Stern 2010)

Consistency of synchrotron and Compton-scattered radiation spectrum with external photon field?

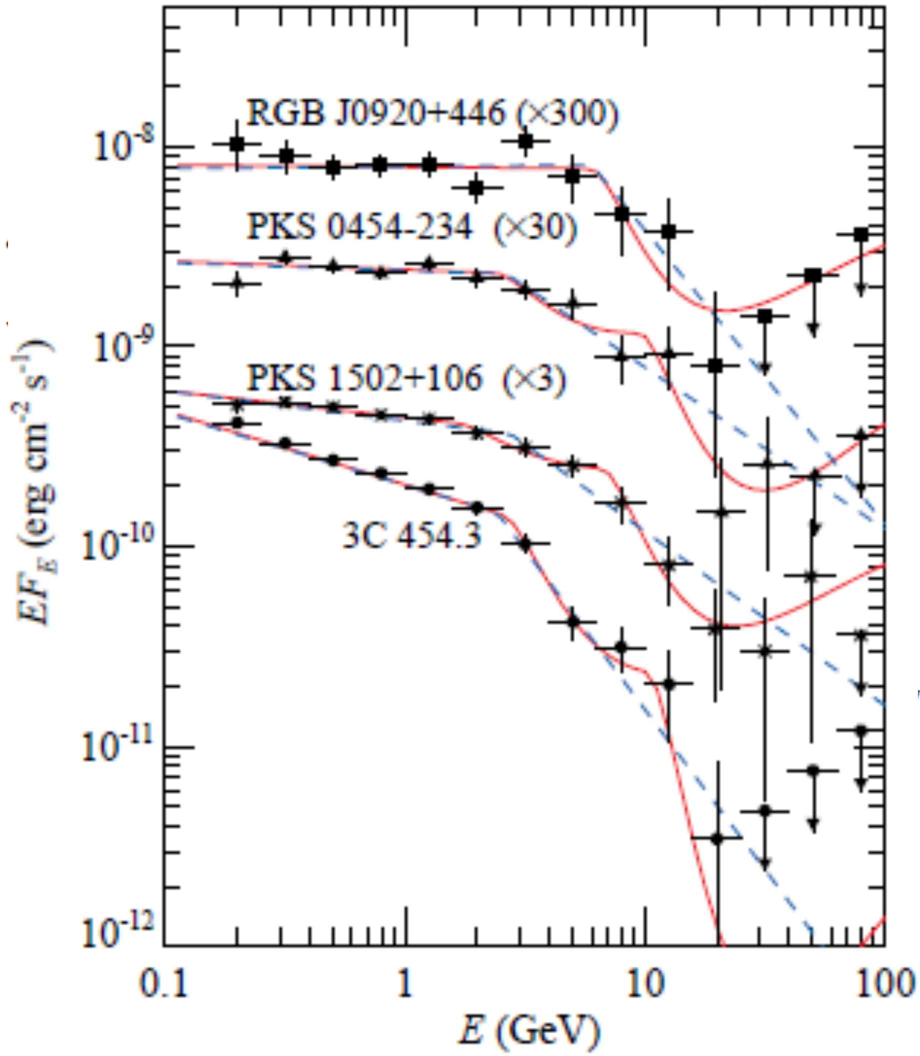

Break due to Compton-Scattered Ly α Radiation?

$$E_{KN}(GeV) \approx 2.1\,GeV / E_*(10.2\,eV)$$

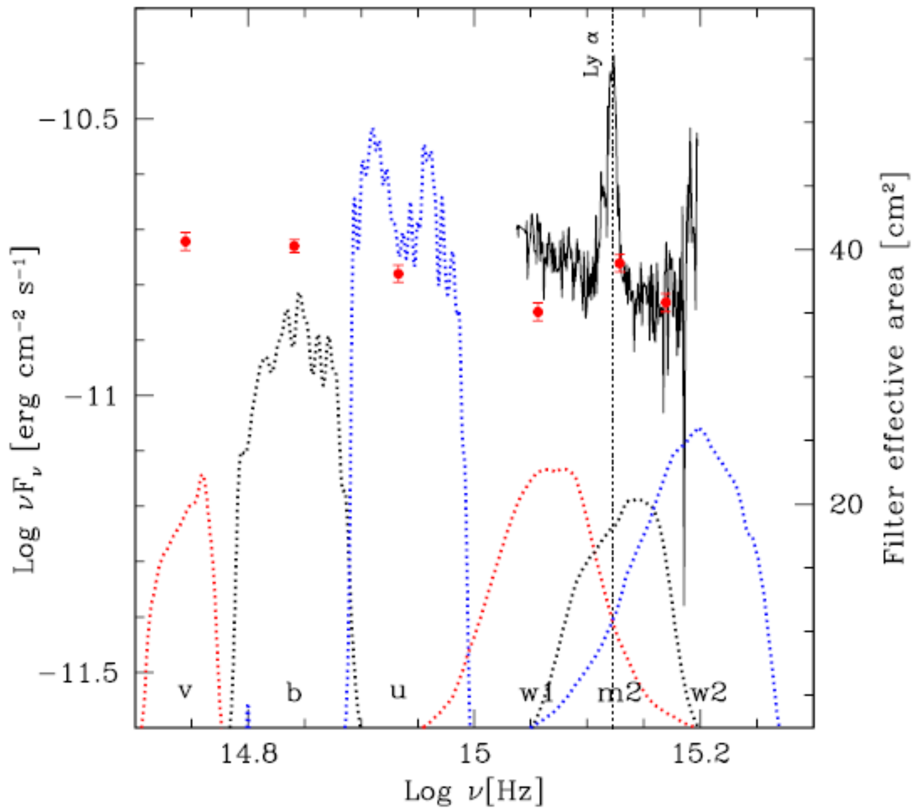

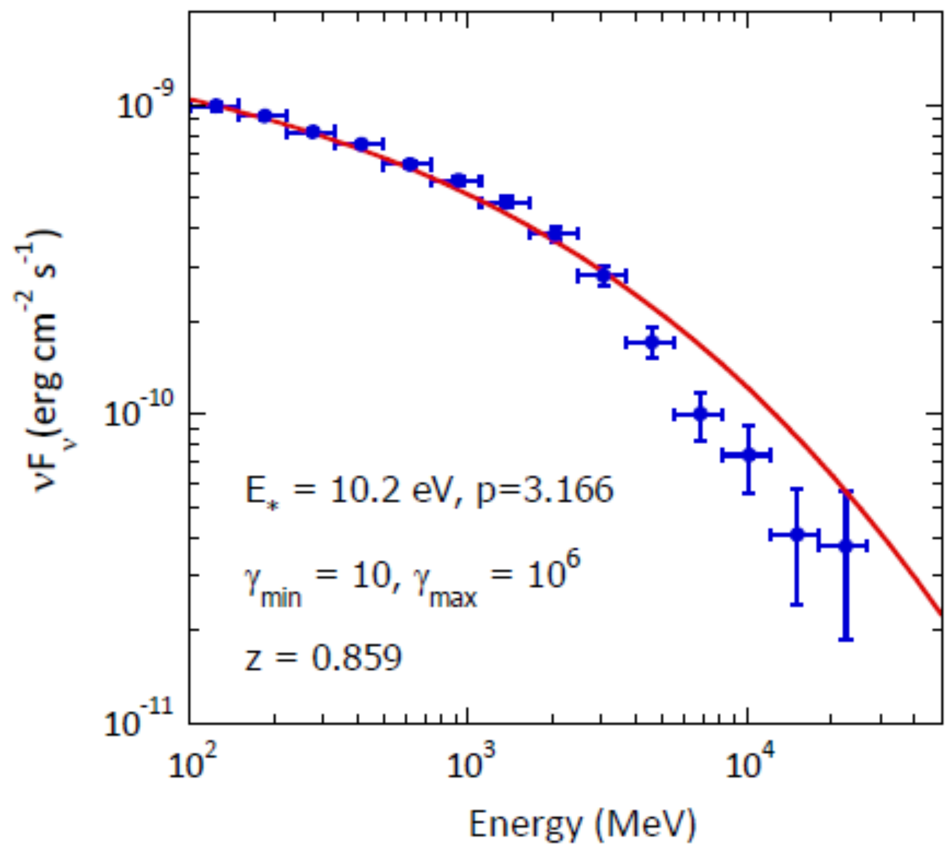

Bonnoli et al. (2009)
GALEX and UVOT observations of strong Ly α: 2×10^{45} erg s^{-1}
Emission region size from reverberation mapping studies
⇒ Energy density of BLR

(cf. Georganopoulos et al. 2001)

VARIABILTY *Hyper-variable*

μεταβλητή

PKS 2155-304

- X-ray selected BL Lac
- $z = 0.116$, $d_L = 540$ Mpc
- Detected by EGRET, AGILE
- August 2006: bright flares, detected by
  - **Swift (Foschini et al. 2007) (3 ks/day)**
  - **HESS (Aharonian et al. 2007)**
    - Variability timescale: ~5 minutes
- BeppoSAX observed variability ~ 1 hr (Zhang et al. 2002)

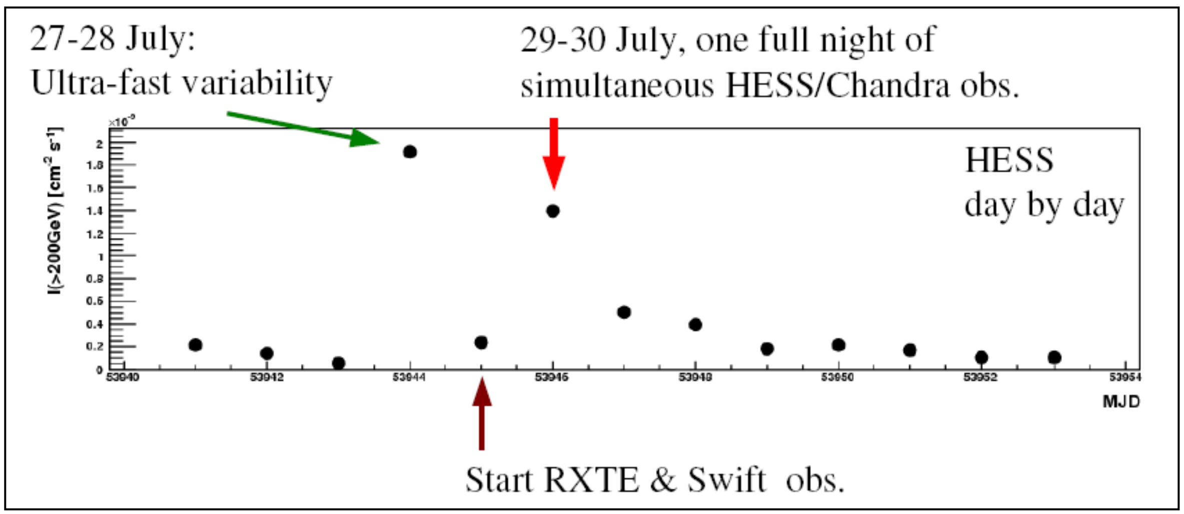

Temporal Variability

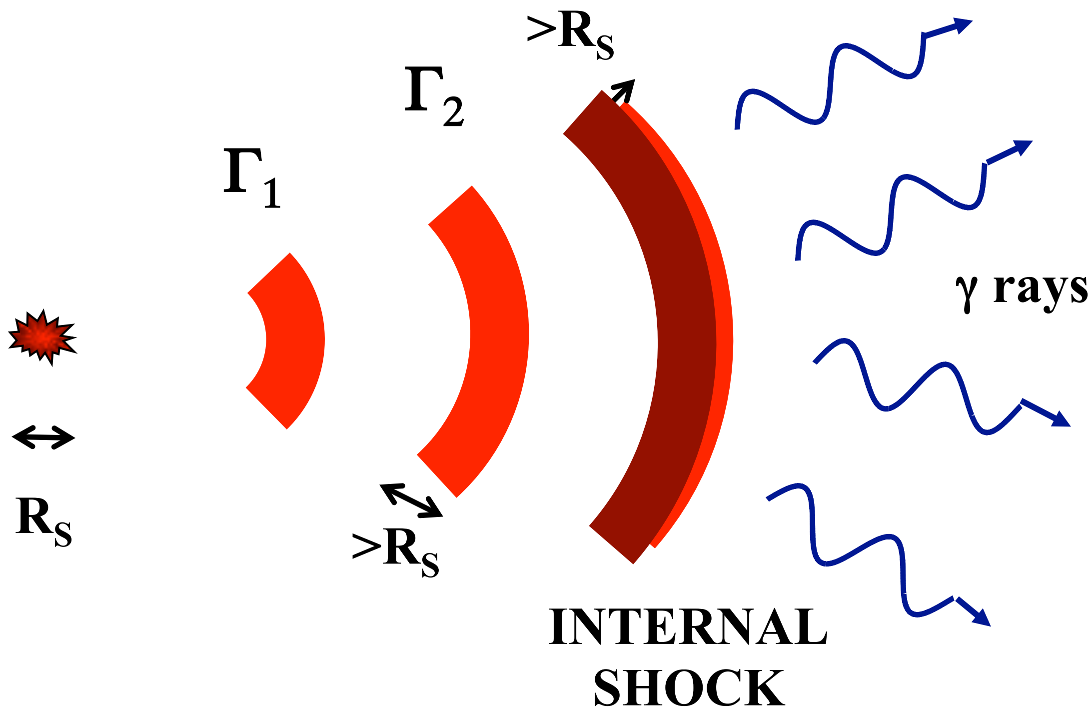

$$R_S = \frac{2GM}{c^2} < \frac{ct_{var}}{(1+z)}?$$

Mini-jets

Magnetically-dominated jets

Size scale in stationary frame: $\Delta R > R_S$
Size scale in comoving frame: $\Delta R' = \Gamma\Delta R > \Gamma R_S$
(Lorentz contracted to size R in stationary frame)

$$t'_{var} > \Delta R'/c > \Gamma R_S/c$$

$$t_{var} = t'_{var}/\Gamma \approx R_S/c$$

Can small-opening angle colliding shells avoid this problem?

Colliding Shell Solution:

1. Variability
2. Unification
3. Light curves
4. UHECR acceleration

3C 279

- Where are the γ-rays made?
- Monitor long-term behavior of light curve
- Correlates with changes in optical polarization and flux
- Highly ordered magnetic field over long timescale
- γ ray dissipation location at multi-pc scale?

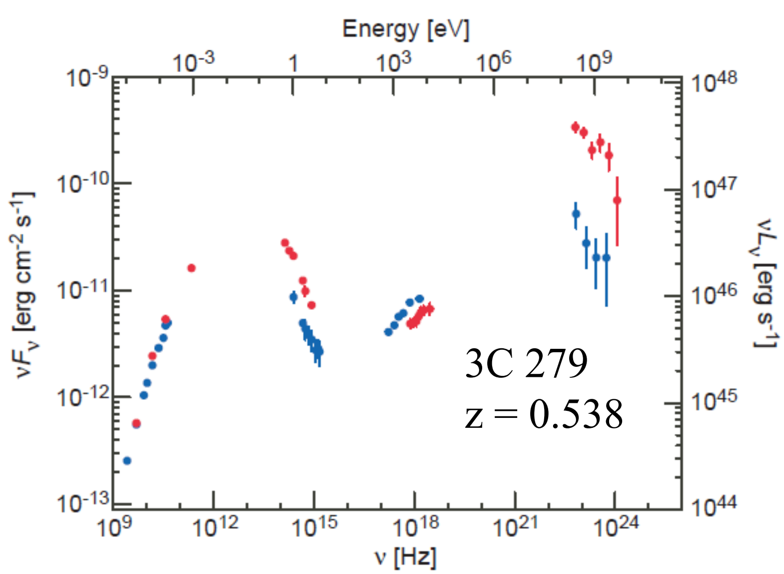

Abdo., et al. 2010, Nature, 463, 919

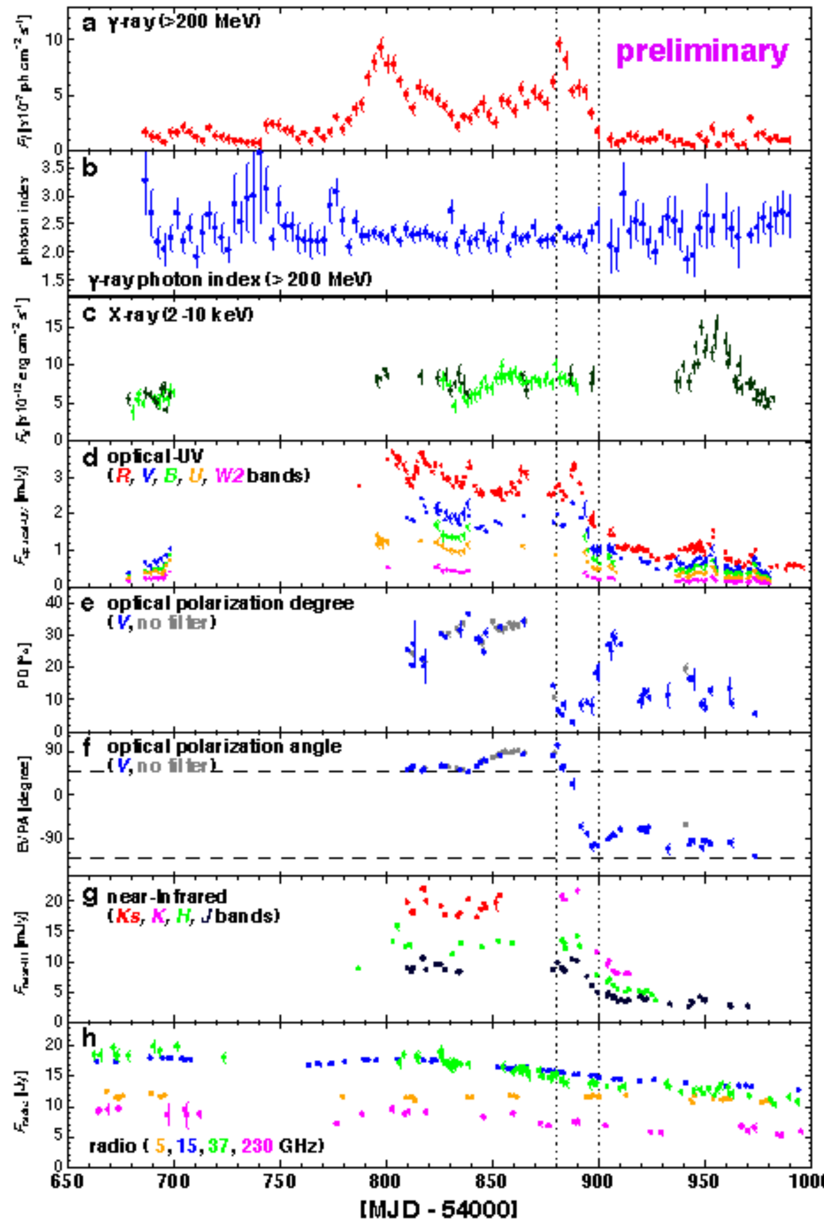

VHE γ rays from Flat Spectrum Quasars

- 3C 279 (z = 0.536) with MAGIC
- PKS 1510-089 (zz = 0.361) with HESS
- PKS 1222+216 (z = 0.432) with Fermi, HESS, VERITAS

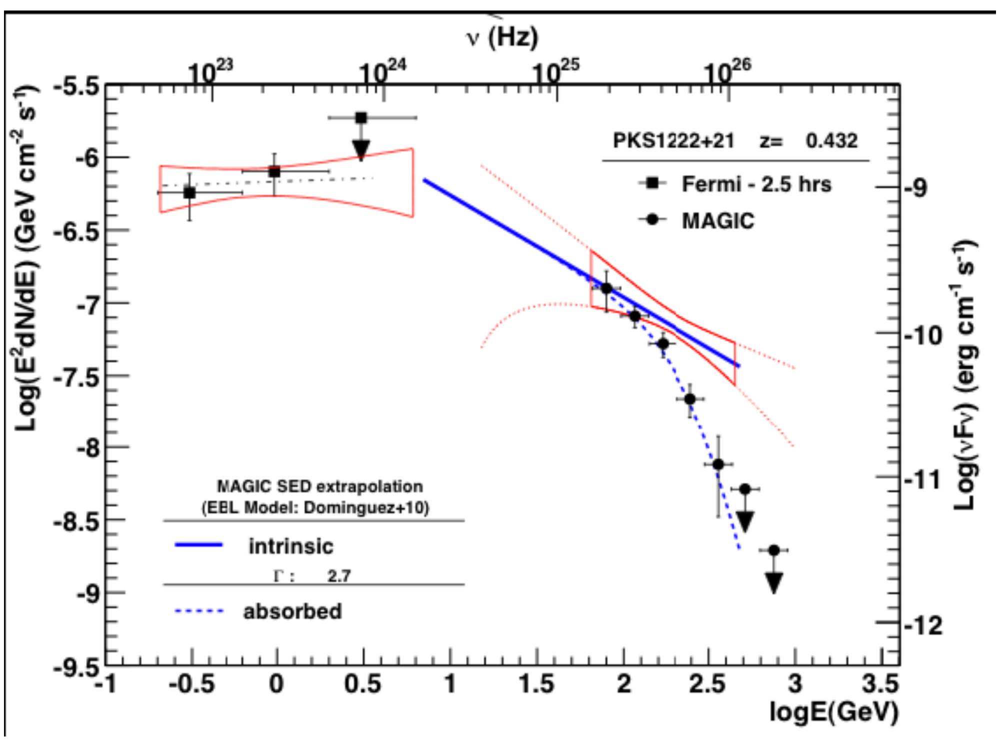

Aleksic et al. (2011)

Variability of 70 – 400 GeV radiation on 10 min timescale

Two-zone scenario

(Tavecchio et al. 2011)

Strong nuclear pc-scale IR emission
(T = 1200 K, L_{IR} = 8x10^{45} erg/s)
Malmrose et al. (2011)

Cosmic-ray induced emission on pc scale

Exercise 1:
Synchrotron/SSC model in the Thomson regime

Can measure 6 defining quantities for syn/SSC model:

z, t_v

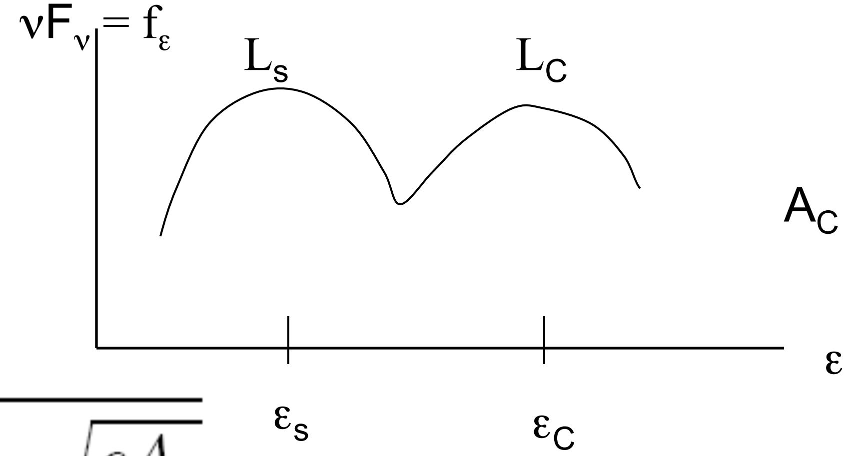

$A_C = L_C/L_s$

$$\Gamma \cong \frac{1}{\epsilon_s}\sqrt{\frac{\epsilon_C}{ct_v B_{cr}}\sqrt{\frac{2L_s}{cA_c}}}$$

$$B \cong \frac{(1+z)B_{cr}\epsilon_s^3}{\epsilon_C^{3/2}}\sqrt{ct_v B_{cr}\sqrt{\frac{cA_c}{2L_s}}}$$

(Ghisellini et al. 1996)

$\Gamma > \Gamma_{min}$

$$B_{cr} = m_e^2 c^3/e\hbar \cong 4.414 \times 10^{13}\ \mathrm{G}$$

Thomson regime $\epsilon_C \epsilon_s \lesssim \left(\frac{\Gamma}{1+z}\right)^2$

Exercise 2:
Nonthermal Electron Synchrotron/SSC model

If electrons are assumed to radiate the observed synchrotron νF_ν spectrum, then in the δ-function approximation for synchrotron emissivity

$$f_\epsilon^{syn} = \frac{\delta_D^4 \epsilon' L'(\epsilon')}{4\pi d_L^2},\ \epsilon' L'(\epsilon') \cong \frac{4}{3} c\sigma_T \frac{B'^2}{8\pi}\gamma'^2 \times \gamma' N_e'(\gamma')$$

$$\epsilon' \cong \frac{B'}{B_{cr}}\gamma'^2, \quad \epsilon \approx \frac{\delta_D \epsilon'}{1+z} \Rightarrow \gamma' \cong \sqrt{\frac{(1+z)\epsilon B_{cr}}{\delta_D B'}}$$

Construct synchrotron/SSC model in δ-function approximation

Relativistic jet physics

New results on blazars and radio galaxies:

1. LBAS / 1LAC/ 2LAC catalogs
2. Multi-GeV spectral softening in FSRQs, LBLs, IBLs; not XBLs
3. Multiwavelength quasi-simultaneous SEDs including GeV emission for radio galaxies, BL Lacs and FSRQse.g.,
   1. FSRQs 3C 454.3, 3C 279
   2. BL Lacs: Mrk 421, PKS 2155-304
   3. Radio galaxies: Cen A, M87, 3C 84
4. 3C 279, PKS 1510-089: location of emission site; complexity of magnetic field
5. Use SED to constrain redshift from EBL model
6. Long (mo – yr) timescale light curves
7. High energy photons from blazar sources: minimum Doppler factor
8. Radio/γ-ray connection

Backup Slides

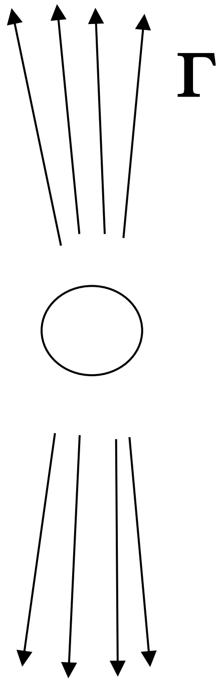

Jet Power

$$n_* = \frac{L^*_{j,ke}}{2\Omega_j R^2(\Gamma m_e c^2)\beta c} = n'(\langle\gamma\rangle + \chi m_p/m_e)$$

$$L^*_B = 2\Omega_j c R^2 \beta \Gamma^2 (\frac{B^2}{8\pi})$$

Total jet power = sum of particle kinetic and magnetic field
Minimum jet power for equipartition (minimum energy) magnetic field
Minimize jet power for measured synchrotron flux

- Jet power: total power available in jet (in observer frame)
- $L_j = 2\pi r_b'\beta\Gamma^2 c(u'_B + u'_p)$ (Celotti & Fabian 1993)
- $dL_j / dB = 0 \rightarrow B_{min}$ (equipartition)
- $B < B_{min} \rightarrow u'_p >> u'_B$ and $f_{SSC} > f_{syn}$

Synchrotron spectrum implies minimum jet power; additionally fitting γ rays gives deviation of model from minimum jet power

Monte Carlo Simulation of Synchrotron/SSC Model

Improved accuracy

Use accurate Compton kernel in the head-on approximation (Compton scattering, *not* inverse Compton scattering)

Mersenne Twister for Random Number Generator

Check uniformity assumption
(cf. Gould 1979)

Can consider non-radial electron distributions

Realistic γγ opacity calculations

High energy tail for EBL studies

Photon conservation

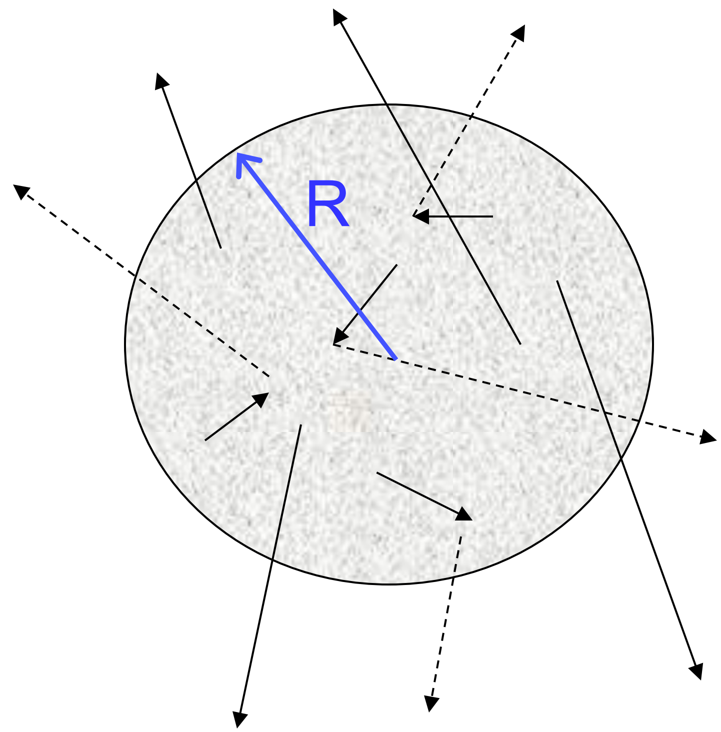

$$\frac{d\sigma_C}{d\epsilon_s} \cong \frac{\pi r_e^2}{\gamma\bar{\epsilon}} \Xi_C \, H(\epsilon_s; \frac{\bar{\epsilon}}{2\gamma}, \frac{2\gamma\bar{\epsilon}}{1+2\bar{\epsilon}})$$

$$\Xi_C \equiv y + y^{-1} - \frac{2\epsilon_s}{\gamma\bar{\epsilon}y} + (\frac{\epsilon_s}{\gamma\bar{\epsilon}y})^2 \qquad y \equiv 1 - \frac{\epsilon_s}{\gamma}$$

$$\bar{\epsilon} = \gamma\epsilon(1 - \cos\hat{\psi})$$

Synchrotron with Photon Conservation

Standard parameters:

$$n_e(\gamma) = k_{eo}\gamma^{-p} H(\gamma;\gamma_1,\gamma_2)$$

$$R = 10^{15}\ cm,\ p = 2.2$$

$$B = 1\ G$$

$$k_{eo} = \frac{n_{eo}(p-1)}{\gamma_1^{1-p} - \gamma_2^{1-p}}$$

$$n_{eo} = 10^{10} cm^{-3},$$

$$\gamma_1 = 10^5, \gamma_2 = 10^6$$

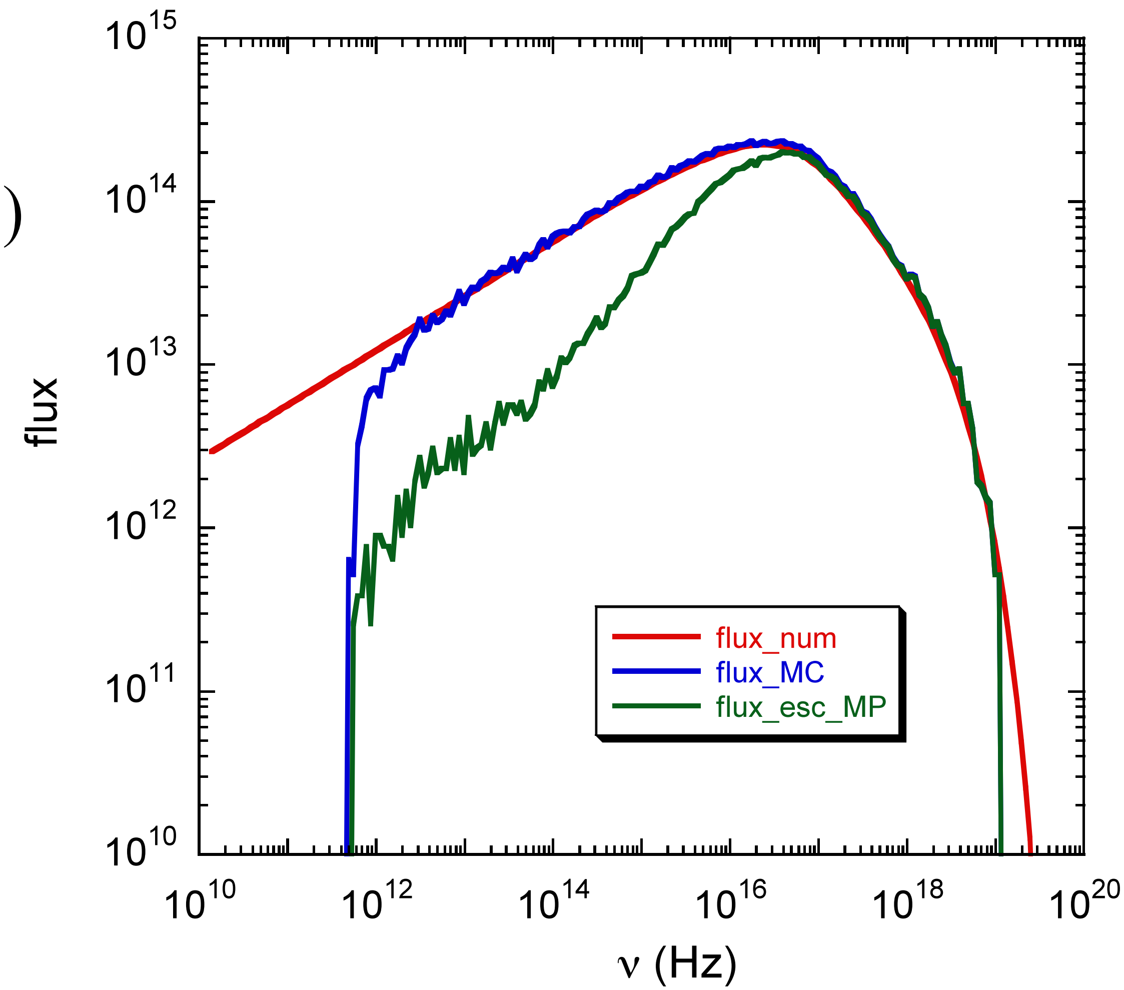

Scattering in KN regime

Solves "line of death" problem in GRB physics?

Monte Carlo Synchrotron/SSC with Uniform Electrons and B-field

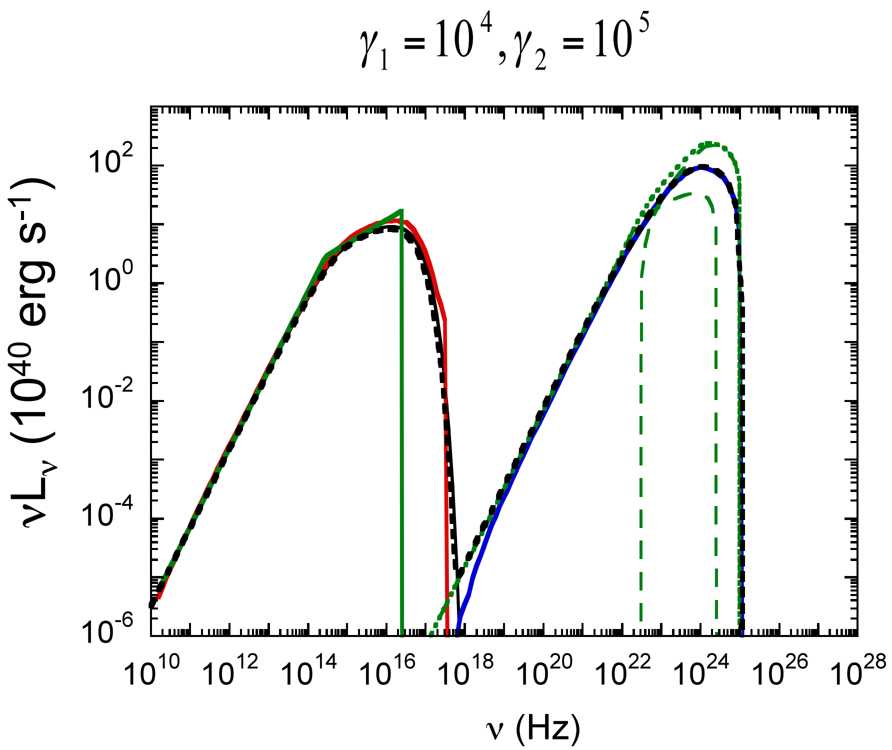

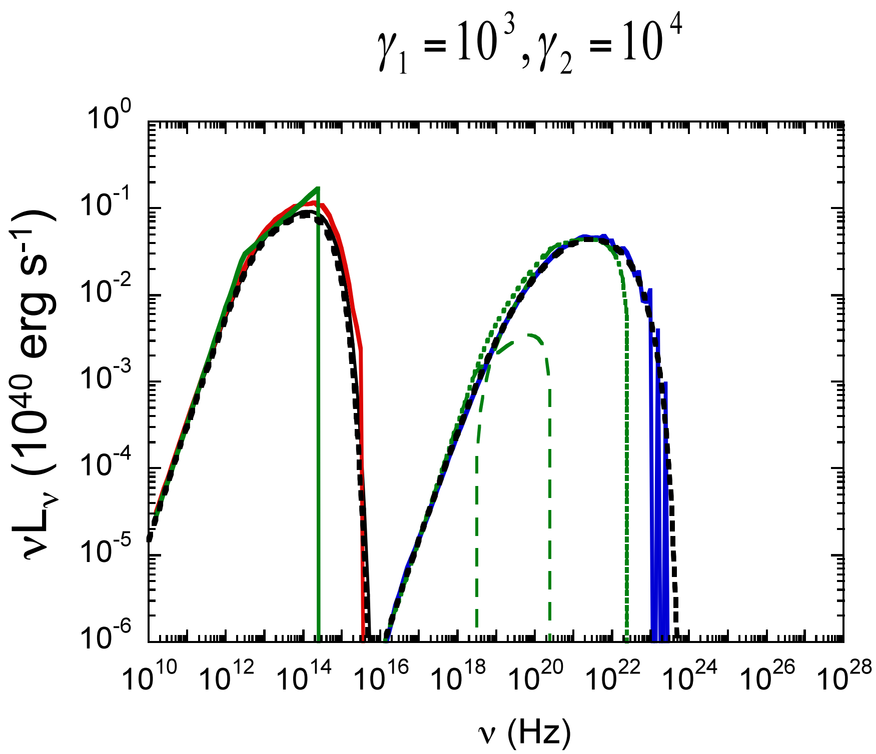

Comparison with δ-function approximation
Discrepancies in amplitude
Discrepancies in high-energy cutoff (could improve it by using exponential cutoff in electron distribution)
Excellent agreement with numerical calculation (mean escape length = 3R/4)

Non-power law spectra

Abdo et al., 2010, ApJ, 710, 1271

- First definitive evidence of a spectral break above 100 MeV
- General feature in FSRQs and many BLLac-LSPs
- Absent in BLLac-HSPs
- Broken power law model seems to be favored
- $\Delta\Gamma \sim 1.0 > 0.5 \rightarrow$ not from radiative cooling
- Favored explanation: feature in the underlying particle distribution
- Implications for EBL studies and blazar contribution to extragalactic diffuse emission

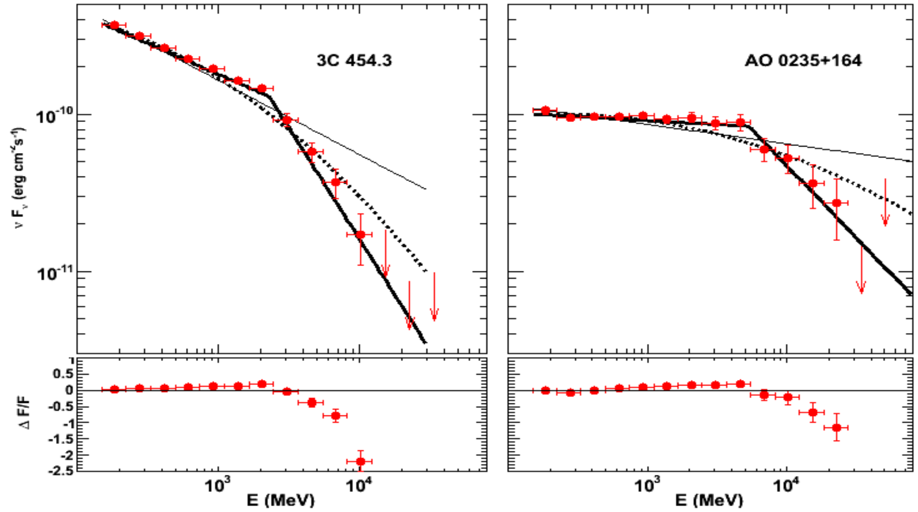

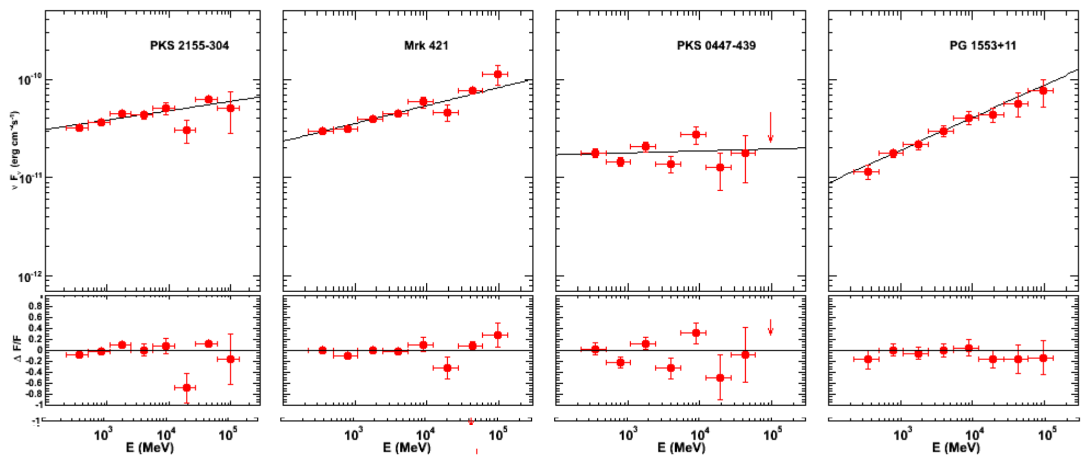

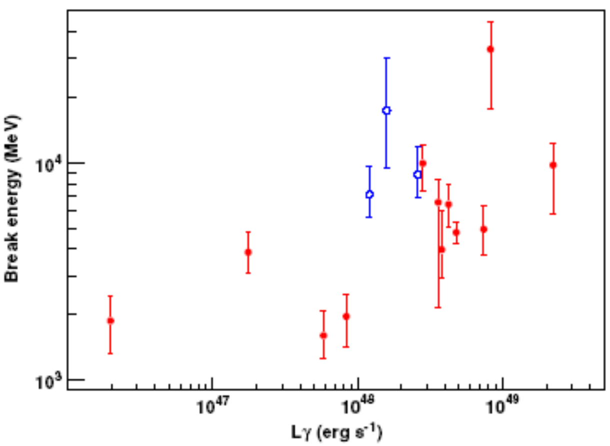

Challenge for modelers to account for the break and the relative constancy of spectral index with time

BL Lac and FSRQ: definition

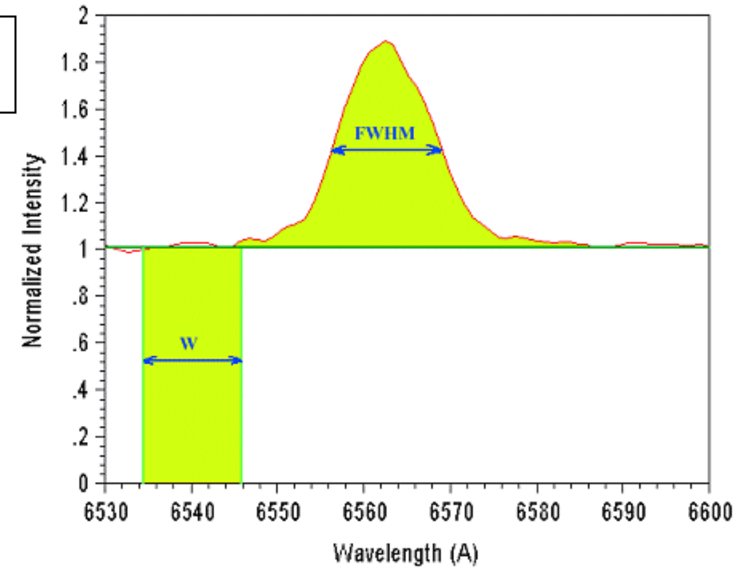

- classify an object as a BL Lac if the equivalent width (EW) of the strongest optical emission line is < 5 Å,

  e.g., [O II] λ3727 and [O III] λ5007

  classification of higher-redshift sources will preferentially use lines at shorter wavelengths (e.g., Lyα λ1216 and C IV λ1549) than for low-redshift sources (e.g., Mg II λ2798 and Hα λ6563).
- a Ca II H/K break ratio C < 0.4,
- Wavelength coverage satisfies $(\lambda_{max} - \lambda_{min})/\lambda_{max} > 1.7$ so that at least one strong emission line would have been detected if it were present.
- Sources for which no optical spectrum or of insufficient quality to determine the optical classification are listed as "unknown type"

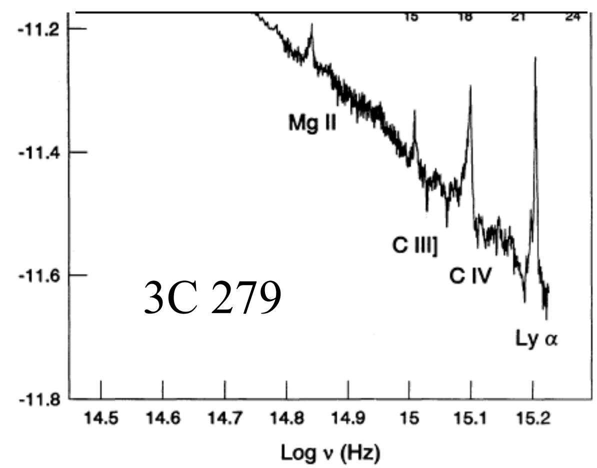

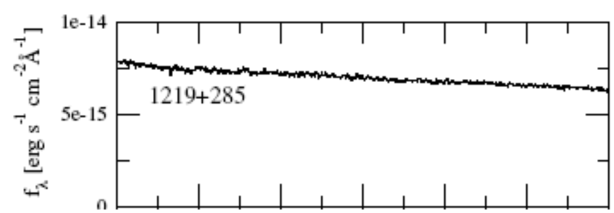

Radio Galaxies and Blazars

FR1/2: radio power/morphology correlation; dividing line at $\cong 4\times10^{40}$ ergs s^{-1}

$\cong$ ($2\times10^{25}h^{-2}_{100}$ W/(Hz-sr) at 178 MHz)

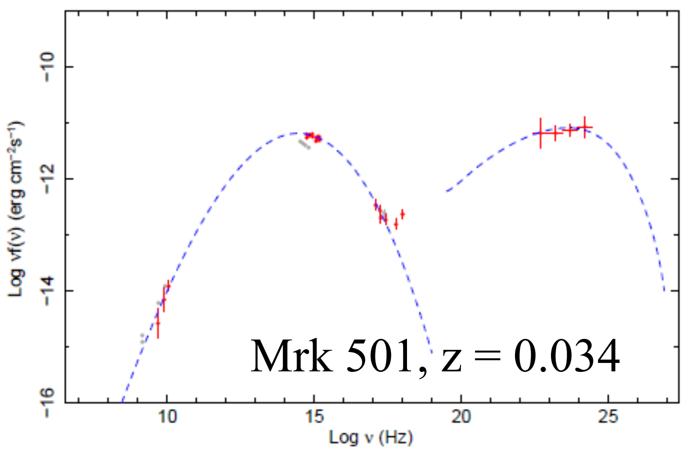

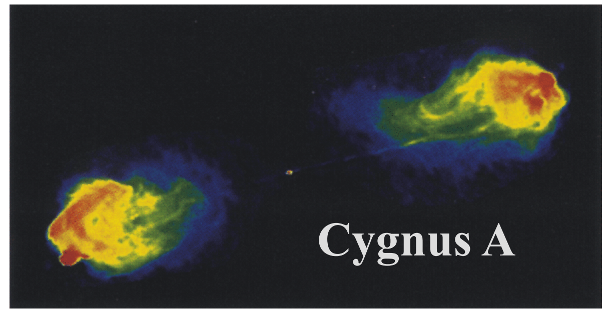

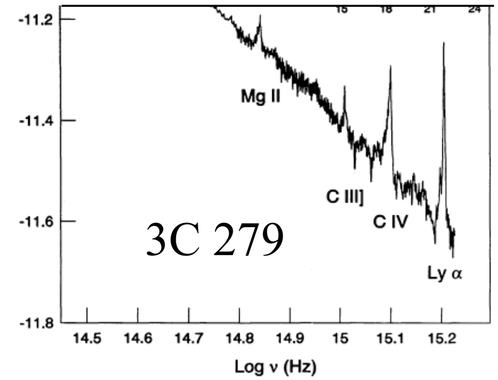

BL Lacs vs. FSRQs:

EW < 5 Å

Ca H-K break < 0.4

$(\lambda_{max} - \lambda_{min})/\lambda_{max} > 1.7$

FR2 ↔ FSRQ

FR1 ↔ BL Lac

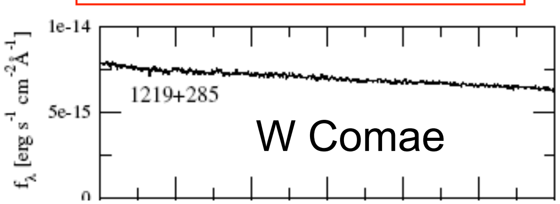

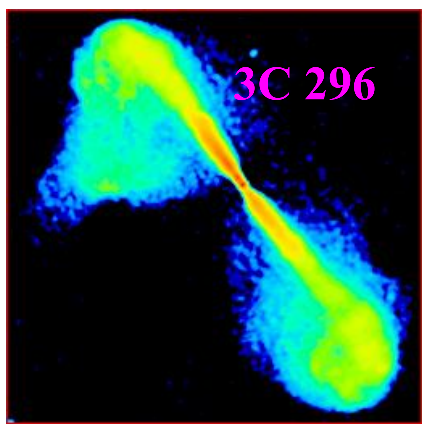

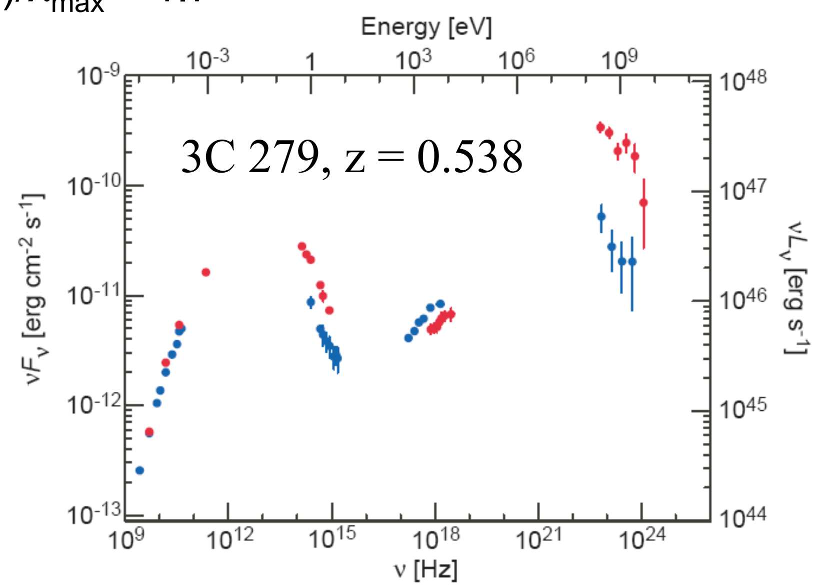

Blazar Unification: Padovani & Urry (1995)

BL Lac vs. FSRQ
RQ vs. RL

Fitting Routine

Code written by Justin Finke

Write SSC as a function of:
δ_D, B, r_b', z, $N_e(\gamma)$.

Use electron spectrum to calculate SSC using Jones (1968) formula

νF_ν^{syn} gives $N_e(\gamma)$
(CS86 expression)

Internal and EBL absorption calculated

Leaves two unknowns to fit:
δ_D and B

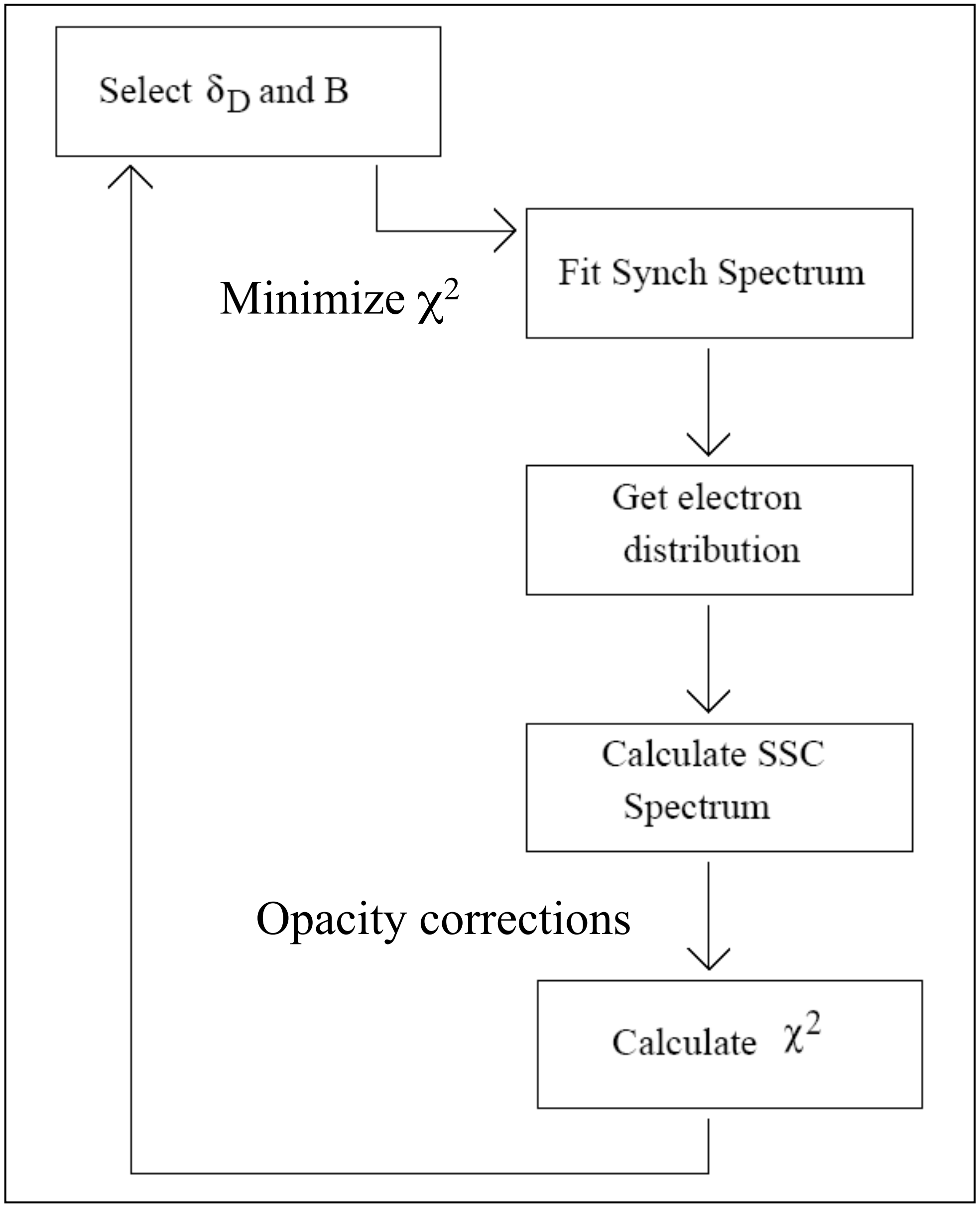

Complex GeV Spectral Behavior

- Sampling separate FSRQ and BL Lac populations

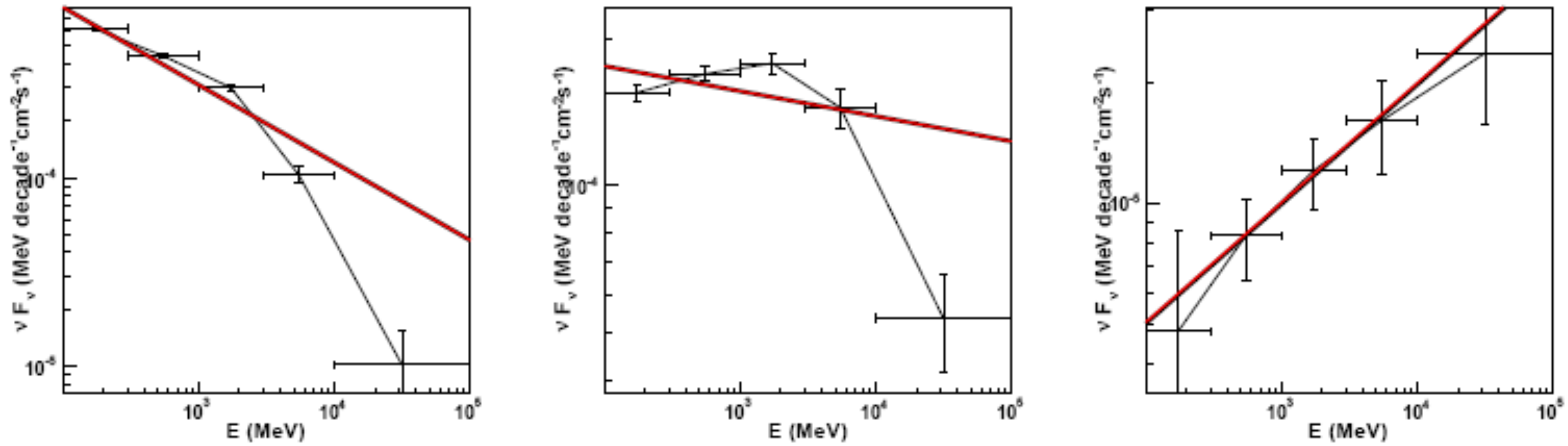

Fig. 14.— SED of 3 bright blazars calculated in five energy bands, compared with the power law fitted over the whole energy range. Left: 3C454.3 (FSRQ), middle: AO 0235+164 (IBL), right: Mkn 501 (HBL)

Abdo et al. (2009) LBAS